

UNIVERSIDADE FEDERAL DO RIO GRANDE DO SUL  
PROGRAMA DE PÓS-GRADUAÇÃO EM ODONTOLOGIA  
DOUTORADO EM ODONTOLOGIA  
ÁREA DE CONCENTRAÇÃO EM PATOLOGIA BUCAL

**NATALIA KOERICH LAUREANO**

**DNA METHYLATION IS A COMMON EVENT THAT REGULATES GENE  
EXPRESSION IN HEAD AND NECK CANCER**

PORTO ALEGRE

2019

UNIVERSIDADE FEDERAL DO RIO GRANDE DO SUL  
PROGRAMA DE PÓS-GRADUAÇÃO EM ODONTOLOGIA  
DOUTORADO EM ODONTOLOGIA  
ÁREA DE CONCENTRAÇÃO EM PATOLOGIA BUCAL

**NATALIA KOERICH LAUREANO**

**DNA METHYLATION IS A COMMON EVENT THAT REGULATES GENE  
EXPRESSION IN HEAD AND NECK CANCER**

Linha de Pesquisa: Câncer Bucal

Tese de Doutorado apresentada ao Programa de Pós-Graduação em Odontologia da Universidade Federal do Rio Grande do Sul, como requisito à obtenção do título de Doutor em Odontologia.

*Área de Concentração: Patologia Bucal*

**Orientador: Prof. Dr. Pantelis Varvaki Rados**  
**Mentora na Alemanha: Dra. Adriana Jou**

PORTO ALEGRE  
2019

*“Coragem,  
A vida é feita de coragem”  
Fernando Haddad*

## ACKNOWLEDGMENTS

Primeiramente, gostaria de agradecer à minha mãe, meu pai e minha irmã, os responsáveis por eu ter chego até aqui;

Ao Meu Bem, por ter sido o meu ombro mais forte durante todo esse processo;

À Xinica, por ter me segurado nos momentos mais difíceis do último ano por e ter sido uma amiga e companheira maravilhosa de trabalho;

À Fer, por todos os conselhos, apoio e orientação desde o mestrado até agora;

Às minhas amigas Vivi, Lele, Nati, Bru e Juju que apesar da distância sempre estavam presente;

À Julia, a melhor surpresa que a pesquisa e a Alemanha me deram;

À Fran e Lauren, minhas eternas amigas e conselheiras;

Às minhas mães alemãs Antje e Nataly por todo amor me dado nos últimos 3 anos;

À Adriana por toda oportunidade, apoio e ter possibilitado o doutorado sanduíche;

À Silvia, pela eterna parceria;

Ao Jochen, por ter me recebido de portas abertas;

Ao Professor Pantelis pela orientação, por ter me aceito e acompanhando nesses últimos 6 anos;

Ao saudoso Professor Manoel, por tanto conhecimento em Patologia;

À querida Marcinha, por todos os bons momentos juntas;

Aos professores da Patologia, por todo ensinamento compartilhado.

Ao Professor Marcelo, pelos ensinamentos em cultura celular e ter me aceito também em seu grupo de pesquisa;

À Lisiane, por estar presente e aberta sempre;

Aos meus colegas da Patologia, transformando os dias de trabalho muito mais agradáveis e divertidos;

À Bibi, Paloma, Leo e Lu, grandes companheiros de experimentos e diversão;

Ao grupo LAMOC por ter me recebido muito bem e me ajudado tanto;

Aos meus colegas do DKFZ e Heidelberg por todo apoio;

À UFRGS, DKFZ e Hospital Universitário de Heidelberg por possibilitarem essa tese;

Às cidades de Porto Alegre e Heidelberg, por terem sido minha casa nos últimos 6 anos.

## ABSTRACT

Head and neck squamous cells carcinoma (HNSCC) represents one of the most prevalent and lethal human malignancies worldwide. Despite the advances in early detection and implementation of interdisciplinary therapy, the aggressive and invasive tumor growth pattern in addition to the resistance to well established treatment modalities, remains the main cause for poor outcome. Thus, a better understanding of molecular features involved in early and late HNSCC steps is an urgent need for the improvement of patients management and outcome. In this study, we utilize multiscale omics based on whole-exome sequencing, global DNA methylation and gene expression profile to investigate cancer-related genes in tumor initiation and progression processes. The combination of genetic and epigenetic alterations showed the effect of DNA methylation in regulating two different genes (RYY2 and SOX2) during tumor initiation and progression. The detection of DNA methylation and respective gene expression might help to predict patients risk for malignant transformation and worse outcome.

**Key-Words:** Head and Neck Carcinoma, DNA methylation, SOX2, RYY2

## SUMMARY

1. INTRODUCTION	08
2. REFERENCES	17
3. GOALS	20
4. SCIENTIFIC ARTICLE I	21
5. CONCLUSION	53

## 1. INTRODUCTION

Head and neck squamous cells carcinoma (HNSCC) is one of the 17 major human cancer types (UHLEN; ZHANG; LEE; SJOSTEDT *et al.*, 2017). HNSCC arises from the malignant transformation of epithelial cells from the oral cavity, oropharynx, larynx and hypopharynx mucosa. The classic risk factors are smoking habit, excessive alcohol consumption and, more recent, infection by high-risk human papillomaviruses (HPVs). HPV infection occurs mainly in oropharynx tumors, and the most prevalent HNSCC subgroup of tumors is of those originated from the oral cavity (OSCC) (FREIER; KNOEPFLE; FLECHTENMACHER; PUNGS *et al.*, 2010; LEEMANS; SNIJDERS; BRAKENHOFF, 2018). With an annual incidence of approximately 600.000 cases worldwide, 15.000 of those in Brazil and Germany alone. HNSCC is one of the most common and lethal human malignancies, representing 350.000 deaths per year (LEEMANS; BRAAKHUIS; BRAKENHOFF, 2011; LEEMANS; SNIJDERS; BRAKENHOFF, 2018; MICHMERHUIZEN; BIRKELAND; BRADFORD; BRENNER, 2016).

During initial diagnosis, most HNSCC patients already present a locally advanced disease which requires complex interdisciplinary therapy consisting of surgery, radiotherapy, and chemotherapy. Despite this highly aggressive approach, which often significantly impairs quality of life, around 50% of patients develop recurrence within 2 years (CITRON; ARMENIA; FRANCHIN; POLESEL *et al.*, 2017) (HADDAD; SHIN, 2008).

Clinical parameters systems, like TNM, currently applied as standard for therapeutic decisions, are unable to predict the tumor biological behavior and consequently fail to predict patients outcome (FREIER; HOFELE; KNOEPFLE; GROSS *et al.*, 2010). In addition, other tumors from head and neck regions with the same origin and diagnosis, such as squamous cells carcinoma, may exhibit different behavior that can not be predicted by their histopathological morphology alone, requiring more detailed genetic and epigenetic profiling (BELBIN; SINGH; BARBER; SOCCI *et al.*, 2002; FREIER; HOFELE; KNOEPFLE; GROSS *et al.*, 2010; LLERAS; SMITH; ADRIEN; SCHLECHT *et al.*, 2013).

Tumor initiation, progression and metastasis of head and neck cancer involve a multistep and multifactorial process resulted from the build-up of DNA-level genetic and epigenetic alterations. The novel, high-throughput technologies have revolutionized the understanding of the genetic and epigenetic processes that drive cancer. The omics studies enable a detailed comprehension of multiple tumor types and their complexity. The cancer genome atlas (TCGA) is a complete database of molecular alterations from 33 cancer types and more than 20.000 primary



samples. A systematic exploration from those omics comprise genomic, epigenomic, transcriptomic and proteomic data (The Cancer Genome Atlas Program - National Cancer Institute, 2018; CIRIELLO; MILLER; AKSOY; SENBABAOGU *et al.*, 2013; DEMOKAN; DALAY, 2011; MARTINCORENA; CAMPBELL, 2015). Thus, a better understanding of molecular features involved in HNSCC during tumor initiation and progression is an urgent need for the improvement of patients management and outcome.

### *Transcription Factors*

Transcription factors are DNA-binding regulatory proteins that influence the recruitment of RNA polymerase II and consequently modulate gene expression. During development and cell differentiation, their activity changes will guide cell-specificity and regulate this process. Alterations in transcription factors can cause different comorbidities such as cardiovascular disease, inflammatory conditions, neurological disorders, diabetes and obesity. In cancer, those alterations are deletion, amplification, chromosomal translocation or mutation that lead to a gain or loss of function of genes that encode transcription factors. Transcription factors are also estimated to be responsible for 20% of oncogenes (PAPAVASSILIOU; PAPAVASSILIOU, 2016).

The SRY-related (*SOX*) transcriptional factor family is composed of 20 gene members, divided in eight groups, *SOXA* to *SOXH*, located at autosomal chromosomes plus the Y chromosome. The *SOX* family is well known for playing a crucial role in different stages of development, physiological, and pathological steps, being responsible for cell type-specific genetic programs in stem, progenitor and highly specialized cells. Due to this important function, modifications on this family, specially mutations are associated with congenital diseases and developmental disorders. Inevitably, somatic mutations or alterations on *SOX* genes will play a role also in cancer development. *SOX* genes are dysregulated in at least one type of cancer, at genetic, epigenetic, transcriptional, translational and post-translational levels, affecting cell stemness, survival, proliferation and migration, and acting as tumor promoter or suppressor depending on tumor type and environment. However, a better characterization of factors responsible for functional regulation of *SOX* genes and proteins is still needed (ANGELOZZI; LEFEBVRE, 2019).

### *SOX2*

*SOX2* belongs to the *SOXB1* group that contains encoding transcriptional activators and is expressed in progenitor cells from embryogenesis to the most specialized adult cells. *SOX2* is one

of the main genes responsible for specification, differentiation and pluripotency maintenance. *SOX2* associated congenital and developmental diseases, characterized by *SOX2* heterozygous loss-of-function, are anophthalmia or microphthalmia syndromes, which comprise craniofacial and skeletal abnormalities, developmental delay, learning difficulties, esophageal atresia, hearing loss and genital abnormalities (ANGELOZZI; LEFEBVRE, 2019).

In cancer, *SOX2* is expressed in 25 different types implicated in tumor growth, tumorigenicity, drug resistance and metastasis of ovary, lung, skin, brain, breast, prostate and pancreatic cancers. In most cancer types, *SOX2* is highly expressed and/or amplified, but the effects of its expression in cancer have only now beginning to be explored and are not yet well clarified (WUEBBEN; RIZZINO, 2017).

*SOX2* is regulated by microRNAs, long non-coding RNAs and post-translational modification. In HNSCC, PI3K/mTOR signaling, the most common activating genetic event in HNSCC, has been shown to regulate *SOX2*, consequently regulating *ALDH1A1* and increasing sphere formation, tumor growth and therapy resistance (KEYSAR; LE; MILLER; JACKSON *et al.*, 2017). While Sharma *et al.*, 2010 showed that loss of *SOX2* induce drug-resistance in cells selected by epigenetic mechanisms (SHARMA; CAO; KUMAR; ZHANG *et al.*, 2018).

Freier *et al.*, 2010, established 20 HNSCC primary cell lines from different anatomic sites to functionally analyze the role of key genes involved in pathogenesis, previously described as relevant clinical signatures by transcriptome analyses, and to better characterize the complexity of HNSCC. By means of chromosomal comparative genomic hybridization (cCGH), the study revealed typical chromosomal aberration in HNSCC primary cell lines. The most frequent aberrations are the copy number gains on autosomal chromosomal arms, especially at the 3q arm where several oncogenes, such as *PIK3CA*, *CCN1*, *FGF12*, *ACK1* and *SOX2*, are located. *PIK3CA* is a well known gene in HNSCC, related to cell survival, proliferation and migration. This gene present genomic amplification and consequent high protein expression in OSCC dysplasias, primary tumors and metastasis. The others oncogenes also play an important role in HNSCC, as *CCN1* is associated with lymph node metastases, *FGF12* with cell survival, and *ACK1* with cell migration and invasiveness (FREIER; HOFELE; KNOEPFLE; GROSS *et al.*, 2010; FREIER; KNOEPFLE; FLECHTENMACHER; PUNGS *et al.*, 2010).

Copy number gain of *SOX2* in OSCC was described before as one of the most frequent chromosomal aberration by the same research group (FREIER; KNOEPFLE; FLECHTENMACHER; PUNGS *et al.*, 2010). Analyzing 40 OSCC samples, they found high amplification levels at the 3q26.33 arm that was directly associated with high *SOX2* mRNA level. This was also the first time

that high expression of *SOX2* was reported in OSCC and underlines *SOX2* as an attractive candidate oncogene to be explored due to the suggestive enrolment in OSCC tumor initiation and progression.

Bayo and Jou et al., 2015 after silencing *SOX2* in HNSCC primary cell lines (FREIER; HOFELE; KNOEPFLE; GROSS *et al.*, 2010) observed an induction of cell motility and a more mesenchymal phenotype of cell lines with amplification on chromosome 3q. The low *SOX2* expression has shown to be an independent prognostic marker for patients with HNSCC. These data suggest that there is an heterogeneous population of cells regarding *SOX2* expression, and tumor cells with high *SOX2* expression due to 3q are more likely of epithelial phenotype, with stem cell characteristics and lower invasive capacity, while cells with 3q gain and low *SOX2* expression developed a mesenchymal phenotype with higher migration and invasive capacities (BAYO; JOU; STENZINGER; SHAO *et al.*, 2015).

The molecular mechanism underlying the regulation of *SOX2* expression in cases with amplification of chromosome 3q is still misunderstood. In this study, we will explore the effect of the most common epigenetic alteration on the regulation of *SOX2* expression in cases with amplification of chromosome 3q.

### *Genetic Alterations*

Genetic alterations are heritable changes that affect the DNA sequence, and are responsible for the change of gene activity or function through mutations, deletions, insertions or translocations in DNA sequence (MOORE; LE; FAN, 2013). They are induced by aging, mutagenic factors, UV light exposure, radiation and oxygen radicals (TAKESHIMA; USHIJIMA, 2019).

### *Copy number alteration*

Copy number alterations (CNAs) are gains or losses of a large region of tumor DNA. Somatic copy-number alterations (SCNAs) affect a larger fraction of the genome in cancers than in any other type of somatic genetic alteration. Those alterations can occur in different levels: focal, arm-level, copy-neutral loss-of-heterozygosity (LOH) and whole-genome duplications (WGD), and play critical roles in activation of oncogenes or inactivation of tumor suppressors (SONG; JI; GLEASON; YANG *et al.*, 2019; ZACK; SCHUMACHER; CARTER; CHERNIACK *et al.*, 2013).

Cancers with the same origin, e. g. SCCs, tended to have similar rates of amplification and deletion in peak SCNA regions. In HNSCC, 43% of SCNA are WGD, and most focal or arm-level

SCNAs amplifications occur after WGD. Amplification is highly associated with gene transcription and expression. Understanding of the biological and phenotypical effects of CNAs has led to substantial advances in cancer diagnostics and therapeutics. Most major cancer types have been systematically profiled for CNAs and CpG methylation, and as a result, many CNAs and DNA methylations have been identified and linked to carcinogenesis and cancer progression (SONG; JI; GLEASON; YANG *et al.*, 2019; ZACK; SCHUMACHER; CARTER; CHERNIACK *et al.*, 2013).

### *Mutation*

DNA mutation is one of the main protagonists in drive cancer development. The changes in DNA sequence take place at base pair or chromosome level. The somatic mutations are alterations that occur in somatic cells and consequently affect only the individual in which the mutations arise. The germline mutations are transmitted by gametes to the next generation.

TP53 is the most mutated gene in the majority of cancer types, followed by MUC16 and MUC4 (LIU; HU; ZHANG; HU *et al.*, 2018). In HNSCC, detection of TP53 mutation is the best predictor for malignant transformation of dysplasia and also for determining surgical margins. The HPV negative tumors presents many mutations, TP53 is the most frequent, followed by CNA loss of CDKN2A and CCND1 (Comprehensive genomic characterization of head and neck squamous cell carcinomas, 2015; LEEMANS; SNIJDERS; BRAKENHOFF, 2018). *PIK3CA* is commonly amplified or mutated in HNSCC activating *PI3K*, and occurs more frequently in HPV positive tumors (KEYSAR; LE; MILLER; JACKSON *et al.*, 2017).

The next-generation sequencing enable detection of rare mutations present in specific cell populations (TAKESHIMA; USHIJIMA, 2019) and might find potential new biomarkers that could help to predict malignant transformation.

### *Epigenetic Alterations*

In contrast to genetic alterations, epigenetic alterations are heritable changes that control gene expression without affecting the DNA sequence. They are responsible for not allowing all genes to be expressed at the same time every cell lineage, leading to diverse gene expression and consequent cell variety and tissue formation. Those changes occur by different mechanisms, the most common being DNA methylation and histone modification (KULIS; ESTELLER, 2010;

MOORE; LE; FAN, 2013; WERNER; KELLY; ISSA, 2017).

Epigenetic alterations are mainly induced by aging, chronic inflammation and smoking history (KLUTSTEIN; NEJMAN; GREENFIELD; CEDAR, 2016; TAKESHIMA; USHIJIMA, 2019). Carcinogen-specific inducers like HBV and HCV infection or alcohol may cause aberrant DNA methylation that can persist even after the inducer is no longer present (TAKESHIMA; USHIJIMA, 2019).

Epigenetic alterations play an important role in all steps of carcinogenesis, from tumor formation to progression and treatment. Consequently, they are interesting targets for cancer detection, diagnosis and stratification, and due to their reversible nature, a promising focal point for development of therapeutical approaches (KULIS; ESTELLER, 2010; WERNER; KELLY; ISSA, 2017).

### *DNA methylation*

The most common epigenetic alteration in the human genome is the DNA methylation. DNA methylation consist in the addition of a methyl group (CH<sub>3</sub>) by a covalent bond to the carbon located in position 5 of a cytosine nucleotide succeeded by a guanine nucleotide forming the CpG units (LLERAS; SMITH; ADRIEN; SCHLECHT *et al.*, 2013). A set of sequenced CpG units concentrated in large clusters is called CpG island (KULIS; ESTELLER, 2010). The CpG islands contains approximately one thousand base pairs, a higher density of CpGs when compared to others parts of the genome. About 50% of gene promoter regions are located in a CpG island (SATO; ISSA; KROPF, 2017), and these locations are preserved throughout evolution due to their important function on gene regulation during development and differentiation, organizing the chromatin structure and transcription factor binding. The methylation of CpG islands leads to gene silencing due to failure of the transcription factor in binding with DNA (MOORE; LE; FAN, 2013).

However, methylation also has an antagonistic function. Like most of CpG units are methylated, when these methylation occur at the gene body, outside the promoter regions, or at enhancer region, there is an increase on gene expression (MOORE; LE; FAN, 2013; WEIGEL; CHAISAINGMONGKOL; ASSENOV; KUHMANN *et al.*, 2019).

The enzymes responsible for establishing and maintaining the methyl group bound to the cytosines are the DNA methyltransferases (DNMT), wich are divided in three known subtypes, DNMT1, DNMT3a and DNMT3b. The most common among them is DNMT1, playing a role in

new DNA methylation and maintenance (KULIS; ESTELLER, 2010; MOORE; LE; FAN, 2013).

The detection of cancer-specific DNA methylation has been useful for diagnostic applications in colorectal, prostate and pancreatic cancer by non-invasive methods based on DNA hypermethylation of cancer-type-specific biomarkers. The hypermethylation status can be used also to predict prognostic and stratify patients with high or low risk in acute myeloid leukemia and breast cancer (WERNER; KELLY; ISSA, 2017).

DNA methylation and gene silencing play an important role in the progression of several cancer types, including HNSCC (CHAISAINGMONGKOL; POPANDA; WARTA; DYCKHOFF *et al.*, 2012). Methylation of promoter regions is a common event on silencing tumor suppressor genes. Promoter methylation of *MGMT* is associated with tumor recurrence and worse outcome, from *DCC* is associated with bone invasion, higher invasiveness capacity and lower survival, and promoter methylation of E-cadherin increases tumor invasion and metastasis in oral cancer. In laryngeal cancer, hypermethylation of *ADAM23* and *DAPK* are associated with tumor progression and lymph node metastasis, respectively (LLERAS; SMITH; ADRIEN; SCHLECHT *et al.*, 2013).

Epigenetic silencing has also been described on other genes linked to HNSCC, such as *CDKN2A*, *LHX6*, *TCF21*, *CEBPA*, *SFRP*, and DNA repair genes *MGMT*, *MLH1*, *MSH2*, *SALL3*, *NEIL1* and *FANCB* (CHAISAINGMONGKOL; POPANDA; WARTA; DYCKHOFF *et al.*, 2012). Promoter hypermethylation of *KIF1A* and *EDNRB* are frequent in primary HNSCC, and have higher DNA methylation than all the others top 10 high methylated genes together. Their detection on saliva samples may provide a potential biomarker by means of non-invasive detection (DEMOKAN; CHANG; CHUANG; MYDLARZ *et al.*, 2010).

The DNA methylation status in head and neck cancer can vary depending on clinical, environmental and genetic characteristics like anatomic site, HPV infection and smoking habits (DEMOKAN; DALAY, 2011). Lleras *et al.*, 2014 showed that HNSCC from different locations (oral cavity, larynx and oropharynx) share common CpG units with epigenetic alterations, i. e. the hypermethylation of *ZNF* genes followed by reduction on gene expression. When compared to their correspondent normal mucosa, those loci showed an increase in DNA methylation, with the oropharynx showing the most prominent. The different anatomic sites also present specific DNA methylation. *UCHL1* is hypermethylated and has a decreased expression in 54% of oral cavity tumors, and the HPV positive cases expressed more than double CpG units methylated when compared to HPV negative in oropharynx, the most significant located on *CDKN2A* loci. The HPV

negative cases were similar in both oral cavity and larynx tumors (LLERAS; SMITH; ADRIEN; SCHLECHT *et al.*, 2013).

Considering the reversible nature of DNA methylation, its frequent occurrence and variability in all stages of tumor development, DNA hypomethylating drugs were developed to reverse DNA hypermethylation and reexpress silenced genes to reprogram cancer cells to a more normal-like state. The FDA approved DNMT inhibitors, 5-aza-2'-deoxycytidine (decitabine (DAC)) and 5-azacytidine (azacitidine (AZA)) have been successfully used to treat myelodysplastic syndrome (MDS). These inhibitors form a covalent bond with DNMT enzymes and the methyl group do not bind to DNA, resulting in genome hypomethylation. The decitabine is DNA specific and azacitidine is DNA while RNA specific. Both drugs must be used in an optimal dose to avoid inhibition of cell proliferation and DNA synthesis, their incorporation into DNA and consequent demethylation effect is cell cycle dependent, shown that repeated exposure with low doses present a better clinical result (CHRISTMAN, 2002; SATO; ISSA; KROPF, 2017).

DAC treatment increased MDS patients survival and progression-free survival when compared to standard treatment, and has also shown effectiveness in leukemia patients resulting in its approval in Europe to treat acute myelogenous leukemia (AML). The applicability of DAC treatment in solid tumors is still a challenge due to the lower drug penetrance and lower proliferative rate when compared to hematological cancer. However, there are evidences of DAC efficiency in inhibit tumor growth *in vitro* and when combined with others chemotherapies in colon cancer cell lines and non-small-cell lung cancer. In HNSCC, DAC have been shown to inhibit DNA methylation and restore gene expression (SATO; ISSA; KROPF, 2017; WERNER; KELLY; ISSA, 2017).

DNA methylation can be assessed by different methods: 1) bisulfite conversion; 2) enzymes with specificity for methylation and unmethylated cytosines; 3) antibodies with specificity for methylated cytosines or 4) nanopore-based single DNA molecule sequencing (WERNER; KELLY; ISSA, 2017). In this study we will analyze DNA methylation status by MassArray, consisting in mass spectrometric analysis of DNA methylation (EpiTyper) combined by bisulfite conversion, *in vitro* transcription and uracil-specific cleavage with mass-spectrometry-based quantification of fragment lengths (Quantitative comparison of DNA methylation assays for biomarker development and clinical applications, 2016).

Thus, the utility of DNA methylation as an interesting target tool may provide promising

clinical applications, development of new biomarker, prediction of therapeutic response and/or prognosis and identification of individuals who may benefit from the therapy (DEMOKAN; DALAY, 2011).

In summary, the malignant transformation of normal cell to cancer cell is due to the accumulation of genetic and epigenetic alterations, but their contribution differ from cancer type and the carcinogens involved. The recent technologies mentioned above, allow for the measurement of those alterations, such as DNA methylation and genetic mutations. The combined analysis of those marks enables a more accurate patient risk assessment, refines diagnostic criteria and prognostic factors to guide treatment decisions. The benefit of target epigenetic modifications is to explore new therapeutic options for patients with significant epigenetic modifications leading to new perspectives in personalized medicine (TAKESHIMA; USHIJIMA, 2019; WERNER; KELLY; ISSA, 2017).



## 2. REFERENCES

- ANGELOZZI, M.; LEFEBVRE, V. SOXopathies: Growing Family of Developmental Disorders Due to SOX Mutations. **Trends Genet**, 35, n. 9, p. 658-671, Sep 2019.
- BAYO, P.; JOU, A.; STENZINGER, A.; SHAO, C. *et al.* Loss of SOX2 expression induces cell motility via vimentin up-regulation and is an unfavorable risk factor for survival of head and neck squamous cell carcinoma. **Mol Oncol**, 9, n. 8, p. 1704-1719, Oct 2015.
- BELBIN, T. J.; SINGH, B.; BARBER, I.; SOCCI, N. *et al.* Molecular classification of head and neck squamous cell carcinoma using cDNA microarrays. **Cancer Res**, 62, n. 4, p. 1184-1190, Feb 15 2002.
- CHSAISINGMONGKOL, J.; POPANDA, O.; WARTA, R.; DYCKHOFF, G. *et al.* Epigenetic screen of human DNA repair genes identifies aberrant promoter methylation of NEIL1 in head and neck squamous cell carcinoma. **Oncogene**, 31, n. 49, p. 5108-5116, Dec 6 2012.
- CHRISTMAN, J. K. 5-Azacytidine and 5-aza-2'-deoxycytidine as inhibitors of DNA methylation: mechanistic studies and their implications for cancer therapy. **Oncogene**, 21, n. 35, p. 5483-5495, Aug 12 2002.
- CIRIELLO, G.; MILLER, M. L.; AKSOY, B. A.; SENBABAOGU, Y. *et al.* Emerging landscape of oncogenic signatures across human cancers. **Nat Genet**, 45, n. 10, p. 1127-1133, Oct 2013.
- CITRON, F.; ARMENIA, J.; FRANCHIN, G.; POLESEL, J. *et al.* An Integrated Approach Identifies Mediators of Local Recurrence in Head and Neck Squamous Carcinoma. **Clin Cancer Res**, 23, n. 14, p. 3769-3780, Jul 15 2017.
- Comprehensive genomic characterization of head and neck squamous cell carcinomas. **Nature**, 517, n. 7536, p. 576-582, Jan 29 2015.
- DEMOKAN, S.; CHANG, X.; CHUANG, A.; MYDLARZ, W. K. *et al.* KIF1A and EDNRB are differentially methylated in primary HNSCC and salivary rinses. **Int J Cancer**, 127, n. 10, p. 2351-2359, Nov 15 2010.
- DEMOKAN, S.; DALAY, N. Role of DNA methylation in head and neck cancer. *In*: **Clin Epigenetics**, 2011. v. 2, p. 123-150.
- FREIER, K.; HOFELE, C.; KNOEPFLE, K.; GROSS, M. *et al.* Cytogenetic characterization of head and neck squamous cell carcinoma cell lines as model systems for the functional analyses of tumor-associated genes. **J Oral Pathol Med**, 39, n. 5, p. 382-389, May 2010.
- FREIER, K.; KNOEPFLE, K.; FLECHTMACHER, C.; PUNGS, S. *et al.* Recurrent copy number gain of transcription factor SOX2 and corresponding high protein expression in oral squamous cell carcinoma. **Genes Chromosomes Cancer**, 49, n. 1, p. 9-16, Jan 2010.

HADDAD, R. I.; SHIN, D. M. Recent advances in head and neck cancer. **N Engl J Med**, 359, n. 11, p. 1143-1154, Sep 11 2008.

KEYSAR, S. B.; LE, P. N.; MILLER, B.; JACKSON, B. C. *et al.* Regulation of Head and Neck Squamous Cancer Stem Cells by PI3K and SOX2. **J Natl Cancer Inst**, 109, n. 1, Jan 2017.

KLUTSTEIN, M.; NEJMAN, D.; GREENFIELD, R.; CEDAR, H. DNA Methylation in Cancer and Aging. **Cancer Res**, 76, n. 12, p. 3446-3450, Jun 15 2016.

KULIS, M.; ESTELLER, M. DNA methylation and cancer. **Adv Genet**, 70, p. 27-56, 2010.

LEEMANS, C. R.; BRAAKHUIS, B. J.; BRAKENHOFF, R. H. The molecular biology of head and neck cancer. **Nat Rev Cancer**, 11, n. 1, p. 9-22, Jan 2011.

LEEMANS, C. R.; SNIJDERS, P. J. F.; BRAKENHOFF, R. H. The molecular landscape of head and neck cancer. **Nat Rev Cancer**, 18, n. 5, p. 269-282, May 2018.

LIU, B.; HU, F.; ZHANG, Q.; HU, H. *et al.* Genomic landscape and mutational impacts of recurrently mutated genes in cancers. *In: Mol Genet Genomic Med*, 2018. v. 6, p. 910-923.

LLERAS, R. A.; SMITH, R. V.; ADRIEN, L. R.; SCHLECHT, N. F. *et al.* Unique DNA Methylation Loci Distinguish Anatomic Site and HPV Status in Head and Neck Squamous Cell Carcinoma. **Clin Cancer Res**, 19, n. 19, p. 5444-5455, Oct 1 2013.

MARTINCORENA, I.; CAMPBELL, P. J. Somatic mutation in cancer and normal cells. **Science**, 349, n. 6255, p. 1483-1489, Sep 25 2015.

MICHMERHUIZEN, N. L.; BIRKELAND, A. C.; BRADFORD, C. R.; BRENNER, J. C. Genetic determinants in head and neck squamous cell carcinoma and their influence on global personalized medicine. **Genes Cancer**, 7, n. 5-6, p. 182-200, May 2016.

MOORE, L. D.; LE, T.; FAN, G. DNA Methylation and Its Basic Function. *In: Neuropsychopharmacology*, 2013. v. 38, p. 23-38.

PAPAVASSILIOU, K. A.; PAPAVASSILIOU, A. G. Transcription Factor Drug Targets. **J Cell Biochem**, 117, n. 12, p. 2693-2696, Dec 2016.

Quantitative comparison of DNA methylation assays for biomarker development and clinical applications. **Nat Biotechnol**, 34, n. 7, p. 726-737, Jul 2016.

SATO, T.; ISSA, J. P. J.; KROPF, P. DNA Hypomethylating Drugs in Cancer Therapy. *In: Cold Spring Harb Perspect Med*, 2017. v. 7.

SHARMA, A.; CAO, E. Y.; KUMAR, V.; ZHANG, X. *et al.* Longitudinal single-cell RNA sequencing of patient-derived primary cells reveals drug-induced infidelity in stem cell hierarchy. **Nat Commun**, 9, n. 1, p. 4931, Nov 22 2018.

SONG, X.; JI, J.; GLEASON, K. J.; YANG, F. *et al.* Insights into Impact of DNA Copy Number Alteration and Methylation on the Proteogenomic Landscape of Human Ovarian Cancer via a Multi-omics Integrative Analysis. **Mol Cell Proteomics**, 18, n. 8 suppl 1, p. S52-s65, Aug 9 2019.

TAKESHIMA, H.; USHIJIMA, T. Accumulation of genetic and epigenetic alterations in normal cells and cancer risk. **npj Precision Oncology**, 3, n. 1, p. 1-8, 2019-03-06 2019. ReviewPaper.

The Cancer Genome Atlas Program - National Cancer Institute. 06/13/2018 - 08:00 2018.

UHLEN, M.; ZHANG, C.; LEE, S.; SJOSTEDT, E. *et al.* A pathology atlas of the human cancer transcriptome. **Science**, 357, n. 6352, Aug 18 2017.

WEIGEL, C.; CHAISAINGMONGKOL, J.; ASSENOV, Y.; KUHMANN, C. *et al.* DNA methylation at an enhancer of the three prime repair exonuclease 2 gene (TREX2) is linked to gene expression and survival in laryngeal cancer. **Clin Epigenetics**, 11, n. 1, p. 67, May 3 2019.

WERNER, R. J.; KELLY, A. D.; ISSA, J. J. Epigenetics and Precision Oncology. **Cancer J**, 23, n. 5, p. 262-269, Sep/Oct 2017.

WUEBBEN, E. L.; RIZZINO, A. The dark side of SOX2: cancer - a comprehensive overview. **Oncotarget**, 8, n. 27, p. 44917-44943, Jul 4 2017.

ZACK, T. I.; SCHUMACHER, S. E.; CARTER, S. L.; CHERNIACK, A. D. *et al.* Pan-cancer patterns of somatic copy number alteration. **Nat Genet**, 45, n. 10, p. 1134-1140, Oct 2013.

### 3. GOALS

Main Goal: Utilize multiscale omics based on whole-exome sequencing, global DNA methylation and gene expression profile to investigate cancer-related genes in tumor initiation and progression of head and neck squamous cells carcinoma.

*Specific Goal 1:* Identify a new regulator gene on the pathogenesis of HNSCC by integrative multiscale omics analysis of somatic mutation and gene promoter methylation through whole-exome sequencing and global DNA methylation (Scientific Article 1).

*Specific Goal 2:* Investigate the role of DNA methylation on the regulation of a well known oncogene, the transcription factor SOX2, by multiscale omics analysis based on gene expression and global DNA methylation, in tumor progression (Scientific Article 2).



## Somatic mutations and promotor methylation of the ryanodine receptor 2 is a common event in the pathogenesis of head and neck cancer

Katrin Schmitt<sup>1</sup>, Britta Molfenter<sup>1</sup>, Natalia Koerich Laureano<sup>1,2,3</sup>, Bouchra Tawk<sup>4</sup>, Matthias Bieg<sup>5</sup>, Xavier Pastor Hostench<sup>6</sup>, Dieter Weichenhan<sup>6</sup>, Nina D. Ullrich<sup>7</sup>, Viny Shang<sup>1</sup>, Daniela Richter<sup>8</sup>, Fabian Stögbauer<sup>9</sup>, Lea Schroeder<sup>10</sup>, Bianca de Bem Prunes<sup>3</sup>, Fernanda Visioli<sup>3</sup>, Pantelis Varvaki Rados<sup>3</sup>, Adriana Jou<sup>1,3</sup>, Michaela Plath<sup>1</sup>, Philippe A. Federspil<sup>1</sup>, Julia Thierauf<sup>1</sup>, Johannes Döscher<sup>11</sup>, Stephanie E. Weissinger<sup>12</sup>, Thomas K. Hoffmann<sup>11</sup>, Steffen Wagner<sup>13</sup>, Claus Wittekindt<sup>13</sup>, Naveed Ishaque<sup>5</sup>, Roland Eils<sup>5</sup>, Jens P. Klussmann<sup>14</sup>, Dana Holzinger<sup>10</sup>, Christoph Plass<sup>6</sup>, Amir Abdollahi<sup>4</sup>, Kolja Freier<sup>15</sup>, Wilko Weichert<sup>16</sup>, Karim Zaoui<sup>1,8</sup> and Jochen Hess<sup>1,16</sup>

<sup>1</sup>Department of Otorhinolaryngology, Head and Neck Surgery, Heidelberg University Hospital, Heidelberg, Germany

<sup>2</sup>Molecular Mechanisms of Head and Neck Tumors, German Cancer Research Center (DKFZ), Heidelberg, Germany

<sup>3</sup>Oral Pathology, Federal University of Rio Grande do Sul (FURG), Porto Alegre, Brazil

<sup>4</sup>Division of Molecular and Translational Radiation Oncology, Heidelberg Ion Therapy Center (HIT), Heidelberg Institute of Radiation Oncology (HIRO), Heidelberg University Hospital, and Translational Radiation Oncology, German Cancer Consortium (DKFZ), National Center for Tumor Diseases (NCT), German Cancer Research Center (DKFZ), Heidelberg, Germany

<sup>5</sup>Division of Functional Bioinformatics, German Cancer Research Center (DKFZ), and Heidelberg Center for Personalized Oncology (DKFZ-HIPO), Heidelberg, Germany

<sup>6</sup>Cancer Epigenetics, German Cancer Research Center (DKFZ), Heidelberg, Germany

<sup>7</sup>Institute of Physiology and Pathophysiology, Division of Cardiovascular Physiology, Heidelberg University, Heidelberg, Germany

<sup>8</sup>Translational Medical Oncology, National Center for Tumor Diseases (NCT) Dresden, Dresden and German Cancer Research Center (DKFZ), Heidelberg, Germany

<sup>9</sup>Institute of Pathology, Heidelberg University Hospital, Heidelberg, Germany

<sup>10</sup>Division of Molecular Diagnostics of Oncogenic Infections, Infection, Inflammation and Cancer Program, German Cancer Research Center (DKFZ), Heidelberg, Germany

<sup>11</sup>Department of Otorhinolaryngology, Head and Neck Surgery, University Medical Center Ulm, Ulm, Germany

<sup>12</sup>Institute of Pathology, University Hospital Ulm, Ulm, Germany

<sup>13</sup>Department of Otorhinolaryngology, Head and Neck Surgery, University of Giessen, Giessen, Germany

<sup>14</sup>Department of Otorhinolaryngology, Head and Neck Surgery, University of Cologne, Cologne, Germany

<sup>15</sup>Department of Oral and Maxillofacial Surgery, Heidelberg University Hospital, Heidelberg, Germany

<sup>16</sup>Institute of Pathology, Technical University Munich (TUM), and German Cancer Consortium (DKTK) partner site, Munich, Germany

Genomic sequencing projects unraveled the mutational landscape of head and neck squamous cell carcinoma (HNSCC) and provided a comprehensive catalog of somatic mutations. However, the limited number of significant cancer-related genes obtained so far only partially explains the biological complexity of HNSCC and hampers the development of novel diagnostic biomarkers and therapeutic targets. We pursued a multiscale omics approach based on whole-exome sequencing, global DNA methylation and gene expression profiling data derived from tumor samples of the HIPO-HNC cohort ( $n = 87$ ), and confirmed new findings with

**Key words:** DNA methylation; HNSCC; RYR2; head and neck cancer; omics analysis

**Abbreviations:** DAC: Docitabine; FFPE: formalin fixed paraffin embedded; HIPO: Heidelberg Center for Personalized Oncology; HNC: head and neck cancer; HNSCC: head and neck squamous cell carcinoma; HPV: human papillomavirus; OPSCC: oropharyngeal squamous cell carcinoma; RYR2: ryanodine receptor 2; TCGA: The Cancer Genome Atlas; TSS: transcription start sites

Additional Supporting Information may be found in the online version of this article.

**Conflict of interest:** All authors declare that they have no conflict of interest.

**Grant sponsor:** NCT Precision Oncology Program (NCT POP), NCT 3.0\_2015.21 (NCT-PRO), Coordination of Improvement of Higher Level Personnel (CAPE); **Grant sponsor:** IMED HNSCC Funding Program of the Helmholtz Initiative on Personalized Medicine; **Grant sponsor:** German Cancer Research Center-Heidelberg Center for Personalized Oncology (DKFZ-HIPO)

\*K.Z. and J.H. contributed equally to this work

**DOI:** 10.1002/ijc.32481

**History:** Received 23 Nov 2018; Accepted 4 Apr 2019; Online 28 May 2019

**Correspondence to:** Karim Zaoui, MD, Department of Otorhinolaryngology, Head and Neck Surgery, Ruprecht-Karls-University, Im Neuenheimer Feld 400, D-69120 Heidelberg, Germany. Tel.: +49-6221-5639510. Fax: +49-6221-5633654. E-mail: karim.zaoui@med.uni-heidelberg.de

datasets from The Cancer Genome Atlas (TCGA). Promoter methylation was confirmed by MassARRAY analysis and protein expression was assessed by immunohistochemistry and immunofluorescence staining. We discovered a set of cancer-related genes with frequent somatic mutations and high frequency of promoter methylation. This included the ryanodine receptor 2 (RYR2), which showed variable promoter methylation and expression in both tumor samples and cell lines. Immunohistochemical staining of tissue sections unraveled a gradual loss of RYR2 expression from normal mucosa *via* dysplastic lesion to invasive cancer and indicated that reduced RYR2 expression in adjacent tissue and precancerous lesions might serve as risk factor for unfavorable prognosis and upcoming malignant conversion. In summary, our data indicate that impaired RYR2 function by either somatic mutation or epigenetic silencing is a common event in HNSCC pathogenesis. Detection of RYR2 expression and/or promoter methylation might enable risk assessment for malignant conversion of dysplastic lesions.

#### What's new?

Multi-scale omics approaches provide a powerful tool to unravel cancer-related genes with the potential to serve as prognostic biomarkers and putative drug targets. This study shows that somatic mutations and epigenetic silencing of the ryanodine receptor 2 (RYR2) are frequent in head and neck cancer. Loss of RYR2 expression was found during transition from dysplastic lesions to invasive tumors. Detection of somatic mutations or promoter methylation might thus improve risk assessment of malignant conversion, which could enable timely and adequate treatment of premalignant lesions.

#### Introduction

Head and neck cancer (HNC) constitutes a heterogeneous group of cancers at the upper aerodigestive tract and is one of the most common malignancies worldwide.<sup>1</sup> In the majority of cases, HNCs are diagnosed as squamous cell carcinoma (HNSCC) originating from the mucosal epithelia of the oral cavity, pharynx or larynx.<sup>2</sup> Cigarette smoking and alcohol abuse are major etiological risk factors for HNSCC, while human papillomavirus (HPV) infection is strongly associated with oropharyngeal cancer risk and prognosis.<sup>3,4</sup>

The standard of care for HNSCC includes surgical excision, radiotherapy and platinum based chemotherapy, which often cause high morbidity and reduced quality of life.<sup>5</sup> Despite multimodal and aggressive treatment regimens, the overall survival of patients with advanced HNSCC remains low due to the high incidence of treatment resistance resulting *in loco*-regional recurrence or distant metastasis.<sup>6,7</sup> Hence, unraveling cellular and molecular principles of intrinsic or acquired treatment resistance has become a prime target for novel drug discovery and design of more effective therapies.<sup>8,9</sup> Equally important is the identification of key players in the pathogenesis of HNSCC, which could improve risk assessment of early malignant conversion to facilitate timely and adequate treatment of premalignant lesions and pave the way to establish new strategies for prevention.

Genomic sequencing approaches have been conducted to unravel the mutational landscape of HNSCC and to provide a comprehensive catalog of candidate genes responsible for the initiation and progression of HNSCC.<sup>10–12</sup> In addition, global gene expression profiling highlighted aberrant activity of gene regulatory networks and signaling cascades, operating in distinct HNSCC subtypes.<sup>13–15</sup>

A fundamental problem of an increasing sample size for cancer genome studies is the large list of putative candidate genes of which many appear highly suspicious on the basis of their

expression pattern, biological function or genomic properties. Most cancer genome studies identified frequent somatic mutations in genes encoding extremely large proteins, such as skeletal or cardiac muscle proteins (e.g., TTN, ryanodine receptor 2 [RYR2] and RYR3), membrane-associated mucins (e.g., MUC16 and MUC4), cytoskeletal dyneins (e.g., DNAH5 and DNAH11) or the neuronal synaptic vesicle protein piccolo (PCLO). New algorithms have been developed to reduce the risk of extensive false-positive findings that overshadow true driver events.<sup>16</sup> However, it is worth noting that the limited number of significant candidate genes or specific mutational hotspots in HNSCC obtained by these tools only partially explains their biological complexity and might hamper the development of novel diagnostic markers and therapeutic targets.<sup>17</sup>

In addition to genomic mutations, the accumulation of epigenetic alterations has been identified as a hallmark of HNSCC. Epigenetic alterations and in particular aberrant DNA methylation of CpG units in the proximity of predicted transcription start sites (TSS) are common features of HNSCC and often result in gene expression silencing and signaling pathway deregulation.<sup>18–25</sup> In many cancers, epigenetic events linked to tumor suppressor gene inactivation through promoter hypermethylation are even more frequent than somatic mutations and could drive neoplastic initiation and malignant progression.<sup>21</sup> So far, only a limited number of studies conducted an integrative approach considering both somatic mutations and gene promoter methylation to unravel new key regulators in the pathogenesis of HNSCC.<sup>22</sup>

#### Materials and Methods

##### Patient material

Patients of the Heidelberg Center for Personalized Oncology-Head and Neck Cancer (HIPO-HNC) cohort ( $n = 87$ ) were treated between 2012 and 2016 at the University Hospital Heidelberg, Germany, and the cohort consists primarily of

advanced HNSCC from the oropharynx ( $n = 36$ , 41.4%), oral cavity ( $n = 22$ , 25.3%), and laryngeal/hypopharyngeal sites ( $n = 18$ , 20.7%, Supporting Information Table S1). Patient samples were obtained under the protocol S 206/2011, approved by the Ethics Committee of Heidelberg University, with written informed consent from all participants. Our study was conducted in accordance with the Declaration of Helsinki. Median age at the time of diagnosis was 61.4 years (range: 39.7–82.5 years), most patients were male ( $n = 67$ , 78.2%) and smokers ( $n = 60$ , 69%). HPV-related tumors were almost exclusively found in the subgroup of oropharyngeal squamous cell carcinoma (OPSCC;  $n = 22$  out of 36, 61.1%), compared to 5.9% ( $n = 3$  out of 51) in non-OPSCC.

Fresh-frozen specimens and tissue sections from formalin fixed paraffin embedded (FFPE) samples of the HIPO HNC cohort were provided by the NCI tissue bank at the Institute for Pathology, University of Heidelberg, Germany in accordance with its regulations and the approval of the Ethics Committee of Heidelberg University. Tissue sections of dysplastic lesions and malignant tumors for the validation cohorts were provided by Departments of Otorhinolaryngology from Ulm and Giessen, Germany and Oral Pathology, Federal University of Rio Grande do Sul, Porto Alegre, Brazil (Supporting Information Table S2) after approval by the local Ethics Committees (Ethics votes: 374/13 and 95/15, CEP UFRGS 237.008).

#### Isolation of analytes

Fresh-frozen tumor samples of the HIPO-HNC cohort were obtained from surgical resection and were evaluated by a pathologist (W.W.) to confirm the diagnosis and to estimate neoplastic cell content. Blood samples were collected prior to surgery. DNA and RNA from tumor specimens and DNA from blood samples were isolated at the central DKFZ HIPO Sample Processing Laboratory using the AllPrep DNA/RNA/Protein Mini Kit (Qiagen, Hilden, Germany) and the QIAamp DNA Blood Mini QIAcube Kit (Qiagen) according to manufacturer's protocols. Quality control and quantification were conducted using a Qubit 2.0 Fluorometer (Thermo Fisher Scientific, Waltham, MA), the Agilent 2100 Bioanalyzer (Agilent Technologies, Santa Clara, CA), and the NanoDrop spectrophotometer (NanoDrop Technologies, Wilmington, DE).

#### Whole-exome sequencing and data analysis

Exome capturing was performed using SureSelect Human All Exon in-solution capture reagents version 4 and version 6 (Agilent Technologies) including UTRs and sequencing was carried out with a HiSeq 2500 instrument (Illumina, San Diego, CA). Mapping of paired end short reads was performed using bwa-aln (version 0.6.2) on the 1,000 genomes project's phase 2 reference sequence ([ftp://ftp.1000genomes.ebi.ac.uk/vol1/ftp/technical/reference/phase2\\_reference\\_assembly\\_sequence/hs37d5.fa.gz](ftp://ftp.1000genomes.ebi.ac.uk/vol1/ftp/technical/reference/phase2_reference_assembly_sequence/hs37d5.fa.gz)) including decoy sequences. Afterward, the Picard software (<https://broadinstitute.github.io/picard/>, version 1.61) was

used to mark duplicate reads. Summary on detected high confidence indels and single nucleotide variant (SNVs) is provided as Supporting Information Tables S3 and S4.

#### Global gene expression profiling

Gene expression profiling was conducted with HumanHT-12 BeadChip arrays (Illumina). Biotin-labeled complementary RNA (cRNA) samples were prepared according to the recommended sample labeling procedure based on the modified Fierwine protocol.<sup>23</sup> In brief, 250–500 ng total RNA was used for cDNA synthesis, followed by an amplification/labeling step to synthesize biotin-labeled cRNA using the Illumina<sup>®</sup> Total Prep<sup>™</sup> RNA Amplification Kit (Life Technologies, Carlsbad, CA) and Biotin-16-UTP (Roche Applied Science, Penzberg, Germany). The cRNA was purified with the Illumina<sup>®</sup> Total Prep<sup>™</sup> RNA Amplification Kit (Life Technologies), following quality control and quantification using the Agilent 2100 Bioanalyzer (Agilent Technologies) and NanoDrop spectrophotometer (NanoDrop Technologies). Microarrays were scanned using an iScan array scanner (Illumina). The raw intensity (IDAT) files were imported into the R environment using the limma package<sup>24</sup> and normalized with the `norm` function<sup>25</sup> with default parameters.

#### Global DNA methylation analysis

DNA concentrations were determined using PicoGreen (Molecular Probes, Eugene, OR) and the quality was confirmed by agarose-gel analysis. Only samples with an average fragment size  $>3$  kb were selected for further analysis. About 500 ng genomic DNA from each sample was bisulfite converted using the EZ-96 DNA Methylation Kit (Zymo Research Corporation, Irvine, CA) according to the manufacturer recommendations. After amplification and enzymatic fragmentation following the instructions in the Illumina Infinium HD Assay Methylation Protocol Guide, samples were applied to Infinium HumanMethylation450 or MethylationEPIC BeadChips (Illumina) and hybridization was performed for 16–24 hr at 48°C. After extension, arrays were fluorescently stained and scanned using an iScan array scanner (Illumina). Data analysis was performed in R studio version 1.1.423 and extraction of beta values was performed using the `minfi` package version 1.24.0.<sup>26–30</sup>

#### MassARRAY analysis

Quantitative DNA methylation analysis by matrix-assisted time-of-flight mass spectrometry (MassARRAY, Agena Bioscience, San Diego, CA) was performed as described previously<sup>3</sup> using primers purchased from Sigma Aldrich and listed in Supporting Information Table S5. We used ClustVis, a freely available web server at <http://bit.cs.ut.ee/clustvis/><sup>32</sup> to analyze and to visualize the MassARRAY data from the HIPO cohort and HNSCC cell lines in a numeric data matrix. Hierarchical clustering was used to generate heatmap plots with calculating all pairwise distances and the color gradient gives an overview of the numeric differences between samples. Objects with the smallest distance are

merged in each step. No scaling was applied to rows and columns represent individual samples, which were clustered using Euclidean distance and average linkage.

#### HPV status

HPV status was determined for all cases by BSGP5+16 +PCR/MPG and E6#1 mRNA detection as described previously.<sup>33</sup> HPV DNA- and RNA-positive cases were considered as HPV-related while all other cases (DNA-negative and DNA-positive but RNA-negative) were considered as non-HPV-related.

#### The Cancer Genome Atlas-HNC and pan-cancer data analysis

The Cancer Genome Atlas (TCGA)-HNC methylation data as assayed by Illumina 450 K Human Methylation Arrays were downloaded in 2015 from the TCGA data portal (<https://tcga-data.nci.nih.gov/tcga/>) for  $n = 279$  patients. Downloaded raw idat files were loaded into R studio version 1.1.423 and preprocessed with minfi version 1.24.0. RYR2 promoter and gene body methylation patterns in normal and tumor samples of 23 TCGA cohorts were analyzed using the MethCNA database (<http://cgma.scu.edu.cn/MethCNA/>).<sup>34</sup> Level 3 RNAseq data were downloaded as described previously.<sup>35</sup> Raw count data were log<sub>2</sub>-transformed using DESeq2 package in R and used for further analysis.<sup>36</sup>

#### Immunohistochemical staining

IHC staining was performed with the Immunodetection Kit (ImmunPRESS HRP Antirabbit, Vector Laboratories, Burlingame, CA), according to manufacturer's instructions. Endogenous peroxidase activity was inactivated by incubation of tissue slides with 3% H<sub>2</sub>O<sub>2</sub> for 10 min at room temperature. For antigen unmasking slides were boiled for 10 min in 10 mM Citrate buffer. Immunostaining was performed with the anti RYR2 antibody (PA5-38329, Thermo Fisher, Waltham, MA) using the DAB peroxidase substrate (Vector Laboratories) and histological staining with hematoxylin was done to visualize tissue architecture. Slides were mounted with Eukitt (Sigma, St Louis, MO). Quantification of the relative number of RYR2-positive cells was done by three independent evaluators based on microscopic inspection and categorized as Score 1: 0% positive, Score 2: 1–33% positive cells, Score 3: 34–66% positive cells and Score 4: ≥67% RYR2 positive cells.

#### Cell culture experiments

HaDu, Cal27, SCC4, SCC9 and SCC25 cells were purchased from the American Type Culture Collection (ATCC, <https://www.lgcstandards-atcc.org/>). All cell lines were cultured in Dulbecco's Modified Eagle's Medium (DMEM, Sigma) supplemented with 10% fetal calf serum (Sigma), 2 mM L-glutamine (Sigma) and 50 µg/ml Penicillin–Streptomycin (Sigma) in a humidified atmosphere with 6% CO<sub>2</sub> at 37°C. Cell cultures were routinely screened to exclude mycoplasma contamination (Venor<sup>®</sup>GeM Classic Mycoplasma Detection Kit; Minerva

Biolabs, Berlin, Germany) according to manufacturer's instructions, and authentication was confirmed by the Multiplex Human Cell Line Authentication Test (Multiplexion, Supporting Information Data S1).

#### Immunofluorescence staining

Cells were seeded on coverslips in 12-well plates (Greiner Bio-One) and were either kept for 48 hr under normal growth conditions or were treated for 72 hr with DMSO or 1 µM Decitabine (DAC, Sigma). Cells were fixed with 4% PFA for 15 min at 4°C, incubated for 30 min in 0.5% Triton X-100 and blocked for 30 min with T-buffer (0.2% Tween 20, 1% BSA in PBS). Cells were incubated for 1 hr at room temperature with the anti-RYR2 antibody (Thermo Fisher, PA5-38329; dilution 1:200 in T-buffer), followed by incubation for 30–60 min with the secondary antibody (Jackson Immuno Research, 111-165-008; dilution 1:200 in T buffer). Nuclei were visualized with DAPI (Sigma, dilution 1:1000). Coverslips were mounted with VectaMount (Vector Laboratories) and were analyzed by fluorescence microscopy (Olympus BX-50F). Pictures were taken from at least five individual fields per experiment using the Olympus XC30 camera. Cells with a perinuclear and dot-like staining pattern were counted manually as RYR2-positive and divided by the total amount of cells to calculate the relative fraction of RYR2-positive cells.

#### Quantitative RT-PCR analysis

Total RNA isolation was performed with the RNeasy Mini Kit (Qiagen) following the manufacturer's instructions. For DNase digestion RNase free DNase Set (Qiagen) was used. Quantity and quality of isolated total RNA were determined with the Nanodrop 2000 Spectrophotometer (Thermo Fisher). For cDNA synthesis, RevertAid First Strand cDNA Synthesis Kit (Thermo Fisher) was used. About 1 µl Random Hexamer Primer was added to 1 µg RNA diluted in 11 µl RNase free water and the mixture was incubated for 5 min at 70°C followed by 5 min at 4°C. Subsequently, 4 µl five times Reaction Buffer, 2 µl 10 mM dNTPs, 1 µl RiboLock RNase Inhibitor and 1 µl RevertAid Reverse Transcriptase were added and incubated for 60 min at 42°C. Quantitative RT-PCR (RQ-PCR) was performed using 10 ng cDNA and the SYBR Green PCR Mix (Thermo Fisher) in the 7900HT Fast Real-Time PCR System (Applied Biosystems, Foster City, CA) according to manufacturer's instruction. RYR2 primers were purchased from Qiagen (RYR2: QuantiTect Primer Assay, Qiagen) and amplification of LMNB1 was used as an internal reference (LMNB1 For: GCTGCTCCTCAACTATGCTAAGAA; LMNB1-Rev: TTTGACGCCAGAAATCCAC). The cycle of threshold (CT) for RYR2 was normalized to the CT value of LMNB1 using the  $\Delta\Delta CT$  method. For each primer, efficiency was determined by a dilution series from 0.01 to 100 ng cDNA from SCC4 cells.

#### Calcium imaging

About 200,000 SCC4 cells were seeded on 35 mm glass bottom dishes (MatTek) and cultured in DMEM for 2 days. Cells were



loaded with 5  $\mu\text{M}$  of the  $\text{Ca}^{2+}$ -sensitive fluorophore Fluo-4-AM (Thermo Fisher) for 20 min at room temperature in Tyrode's solution (140 mM NaCl, 5.4 mM KCl, 1.8 mM  $\text{CaCl}_2$ , 1.1 mM  $\text{MgCl}_2$ , 5 mM HEPES, 10 mM Glucose). Cells were washed with fresh solution and left for 10 min for deesterification before taking videos of cell clusters on a confocal microscope (Olympus IX81 Fluoview1000). Using a 60 $\times$  water immersion objective (1.2 numerical aperture), images were continuously recorded at a resolution of 512 $\times$ 512 pixel and a rate of 2  $\mu\text{s}$  per pixel to collect 100–160 images. Cytosolic  $\text{Ca}^{2+}$  signals were recorded at resting conditions and during stimulation with 10 mM Calcein (Sigma) with or without 5 min preincubation with 10  $\mu\text{M}$  Ryanodine (Tocris), a potent RYR2 antagonist. Fluo-4 was excited at 473 nm and emission was collected between 490 and 540 nm. Images and videos were processed with ImageJ.<sup>37</sup> Baseline fluorescence intensity was determined independently for each measurement and after subtraction of Caffeine induced  $\text{Ca}^{2+}$  quenching. For each setting, at least three independent areas with more than 50 individual cells in total were examined on single cell level. Relative cytoplasmic  $\text{Ca}^{2+}$  levels are given in  $\Delta F/F_0$  with  $F_0$  as basal  $\text{Ca}^{2+}$  level at rest after background subtraction.

#### Bioinformatics and statistical analysis

SNV calling was performed using an in-house developed workflow based on samtools-mpileup. This workflow was also used in the frame of the ICGC PanCancer project and can be accessed via the Dockstore webpage (<https://dockstore.org/containers/quay.io/pancancer/pcawg-dkz-workflow>).<sup>38–40</sup> In short, the workflow first determines variants in the tumor sample and afterward checks, if these variants are also found in the patient matched control sample to distinguish somatic from germline calls. Further annotation of the variants was done using publicly available tracks, like 1,000 Genome variants, single nucleotide polymorphisms (dbSNP), repeats and other elements. Functional relevance was assessed using the Annovar software, and the variants were scored for confidence.<sup>41</sup> Small insertions and deletions were obtained from Platypus (version 0.7.4) and further annotated and confidence assessed similarly as in SNV calling.<sup>42</sup>

Mutational significance calculation was done using mutSigCV.<sup>10</sup> PCA analysis and illustration by heatmaps were done with <https://bit.cs.ut.ee/clusvis/>.<sup>32</sup> Columns are clustered using Euclidean distance and average linkage. Coding non-synonymous SNVs, which were found in the TCGA HNC and HPC-HNC cohorts, were analyzed with several algorithms (MutationAssessor,<sup>43</sup> MutationTaster,<sup>44</sup> PolyPhen 2,<sup>45</sup> CADD,<sup>46</sup> SIFT,<sup>47</sup> BATHMM<sup>38–40</sup>) to predict the functional consequence of missense variations. Statistical analysis was done using GraphPad (<https://www.graphpad.com/quickcals/index.cfm>) and IBM SPSS Statistics version 25. *p* Values <0.05 were considered statistically significant.

#### Data availability

The data discussed in this publication have been deposited in NCBI's Gene Expression Omnibus (Edgar *et al.*, 2002) and are

accessible through GEO Series accession number GSE117973 (<https://www.ncbi.nlm.nih.gov/geo/query/acc.cgi?acc=GSE117973>) or have been submitted to ArrayExpress (E-MTAB-7478, E-MTAB 7468).

## Results

### Whole-exome sequencing and global DNA methylation analysis

Whole-exome sequencing data were available for 86 patients of the HPC-HNC cohort and revealed 28,322 SNVs and 1,969 InDels in total. The highest frequency for somatic mutations was identified for *TP53* in non-HPV-related tumors (75.8%), while only one HPV related tumor had a *TP53* mutation (Fig. 1a). As expected, frequent somatic mutations were found in several genes (e.g., *TTN*, *MUC16*, *PLO1* and *RYR2*) encoding extremely large proteins. Candidate genes with the highest mutational frequency in the HPC-HNC cohort and a somatic mutation frequency of at least 5% of cases in the TCGA-HNC cohort ( $n = 510$ , <http://www.cbioportal.org/>) were selected for further analysis (Supporting Information Fig. S1).

Gene promoter methylation was assessed by global DNA methylome array analysis and revealed a high beta value (mean and median >0.3) for probes located in the proximity of the predicted TSS for *FAT3*, *TTN*, *MUC16*, *RYR2*, *USH2A*, *PAPPA2*, *ASD1* and *LRP1B* (Fig. 1b). DNA methylation and transcript levels for candidate genes with highest beta values were analyzed for samples of the TCGA cohort ( $n = 279$ ), which confirmed a high correlation for *LAT3*, *MUC16*, *RYR2*, *USH2A*, *PAPPA2* and *LRP1B* (Supporting Information Fig. S2). While high *PAPPA2*, *MUC16* or *FAT3* promoter methylation were positively correlated with their transcript levels, an inverse correlation was detected for *RYR2* or *LRP1B*. In addition, analysis of DNA methylation patterns for normal and tumor samples of the TCGA-HNC cohort by the MethCNA online tool (<http://cgma.scu.edu.cn/MethCNA/>) demonstrated a prominent difference for probes located at the *RYR2* promoter but not in the gene body (Fig. 1c). A pan-cancer analysis with 7,731 tumor samples and 741 controls from 23 TCGA cohorts revealed a prominent difference in DNA methylation of probes annotated for the *RYR2* promoter but not the gene body (Supporting Information Fig. S3A). A more detailed analysis of cancer cohorts for which DNA methylation data were available for at least  $n = 20$  control samples demonstrated that *RYR2* promoter methylation is a common feature for most human cancers analyzed, but is less evident in kidney renal papillary cell carcinoma (TCGA KTRP), kidney renal clear cell carcinoma (TCGA KIRC) or thyroid carcinoma (TCGA-THCA). It is worth noting that these cancers are also characterized by a rather low frequency of somatic mutations in *RYR2* (Supporting Information Fig. S3C). As observed previously for TCGA-HNC, several cancers including prostate adenocarcinoma (TCGA-PRAD), pancreatic adenocarcinoma (TCGA-PAAD) and cervical cancer (TCGA-CECS) exhibit a highly significant and inverse correlation

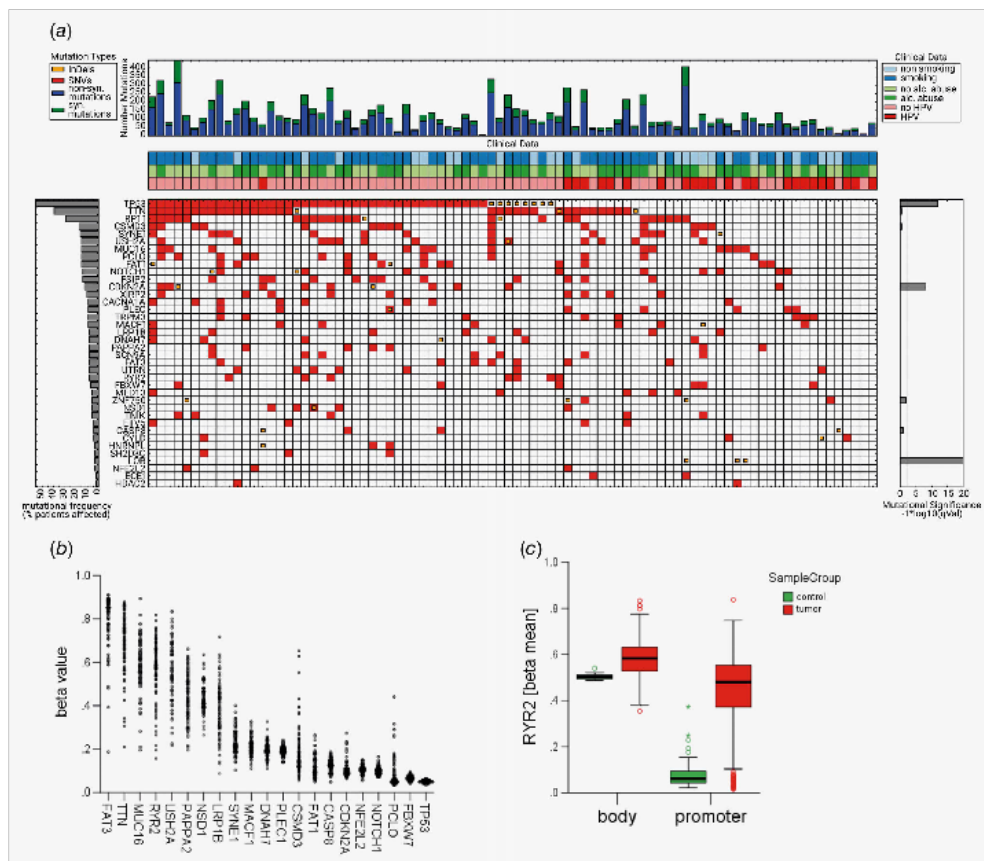


**Figure 1.** Mutational landscape and gene promoter methylation of the HIPO-HNC cohort. (a) OncoPrint indicates the number of somatic mutations per sample, clinical risk factors and mutation types of most frequently affected genes based on whole-exome sequencing data of the HIPO-HNC cohort ( $n = 86$ ). (b) The graph summarizes mean beta values of probes in the proximity of annotated transcriptional start sites for most frequently mutated candidate genes in the HIPO-HNC cohort based on global DNA methylation arrays. (c) Box plot depicts mean beta values for probes located at the *RYR2* promoter or gene body of normal (green,  $n = 50$ ) or tumor samples (red,  $n = 529$ ) from the TCGA-HNC cohort (<http://cgma.scri.edu.cn/MethCNA/>). [Color figure can be viewed at [wileyonlinelibrary.com](http://wileyonlinelibrary.com)]

between gene promoter methylation and *RYR2* transcript levels (Supporting Information Fig. S3B).

#### ***RYR2* promoter methylation and transcription**

Inspection of the *RYR2* promoter using the UCSC Genome Browser revealed a well-defined CpG island and three array probes (cg03422911, cg18375860 and cg19764418) are located at its 5'-region (Supporting Information Fig. S4A). MassARRAY analysis based on six amplicons, which were designed to cover most of the CpG island, was conducted to confirm variable DNA methylation for samples of the HIPO-HNC cohort. Mean values of MassARRAY data for Amplicon 1 and 2 were significantly

correlated with mean beta values of overlapping array probes (Supporting Information Fig. S4B). Hierarchical clustering based on quantitative MassARRAY data revealed two main clusters of samples with low to moderate (Cluster A1 and A2) or high *RYR2* promoter methylation (Cluster B; Fig. 2a and 2b). In line with data from control samples of the TCGA-HNC cohort (Fig. 1c), samples from normal mucosa ( $n = 4$ ) revealed a low methylation value and resemble *RYR2* promoter methylation patterns, which were closely related to HNSCC samples of Cluster A1.

As expected, *RYR2* transcript levels were significantly reduced in cluster B as compared to Clusters A1 and A2 (Fig. 2c). HPV-related tumors were enriched in Clusters A2

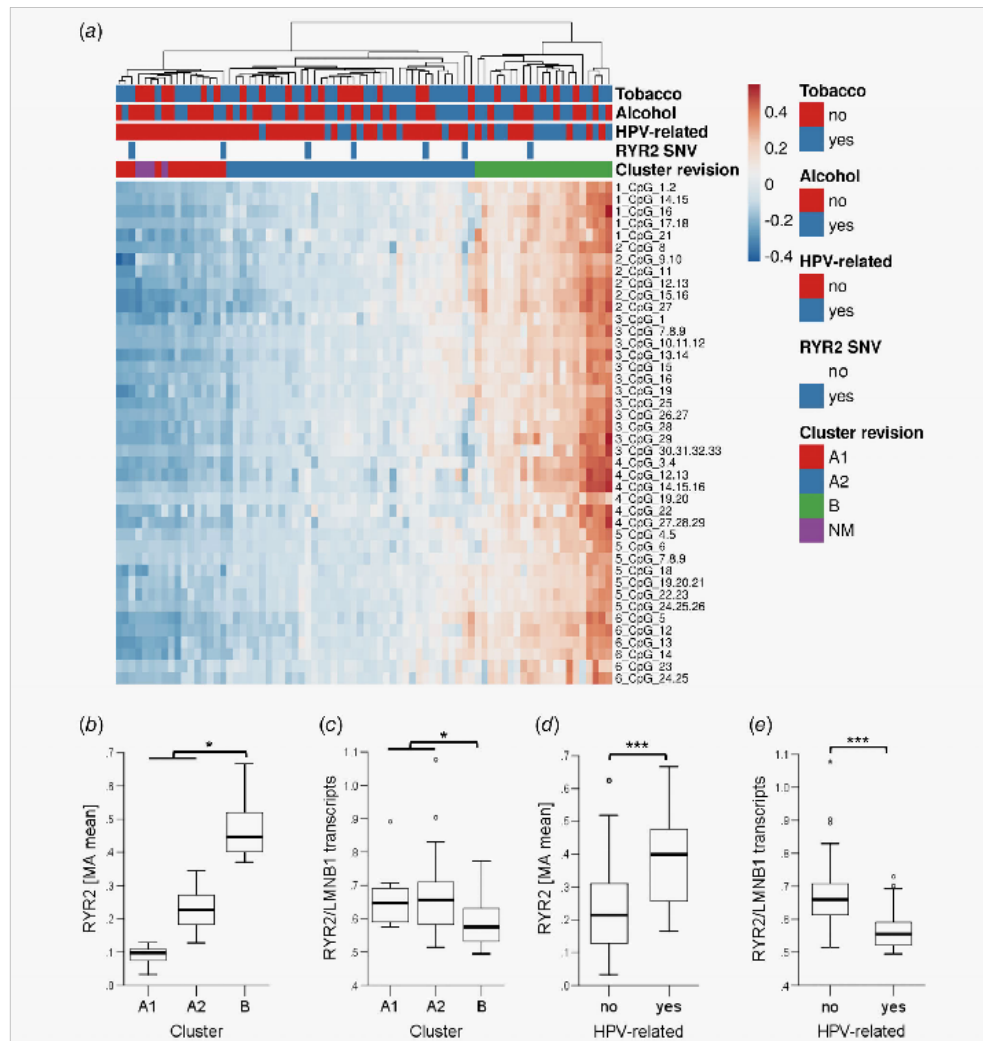


**Figure 2.** *RYR2* gene promoter methylation and expression in the HIPO-HNC cohort. (a) The heatmap was generated by unsupervised hierarchical clustering of MassARRAY data for CpGs (rows) applying Euclidean distance and average linkage on columns (cases of the HIPO-HNC cohort,  $n = 77$ ) and indicates two main clusters (Cluster A and B). Cluster A is further divided into two subclusters A1 and A2. NM, normal mucosa ( $n = 4$ ). Box plots show the distribution of mean MassARRAY values (b) and of relative *RYR2* transcript normalized to LMNB1 transcript levels (c) for samples in cluster A1, A2 and B of the HIPO-HNC cohort as well as the significant differences in *RYR2* promoter methylation (d) and transcript levels (e) between HPV related and non-HPV related tumors. Unpaired t test: \* $p$  value  $< 0.05$  and \*\*\* $p$  value  $< 0.0005$ . [Color figure can be viewed at [wileyonlinelibrary.com](http://wileyonlinelibrary.com)]

and B, and were completely absent in Cluster A1 (Fig. 2a, Supporting Information Table S6). A significantly higher *RYR2* methylation and lower transcript levels were evident in

HPV-related as compared to non-HPV-related tumors of the HIPO-HNC cohort (Figs. 2d and 2e), and was confirmed in the TCGA-HNC cohort (Supporting Information Fig. S5).

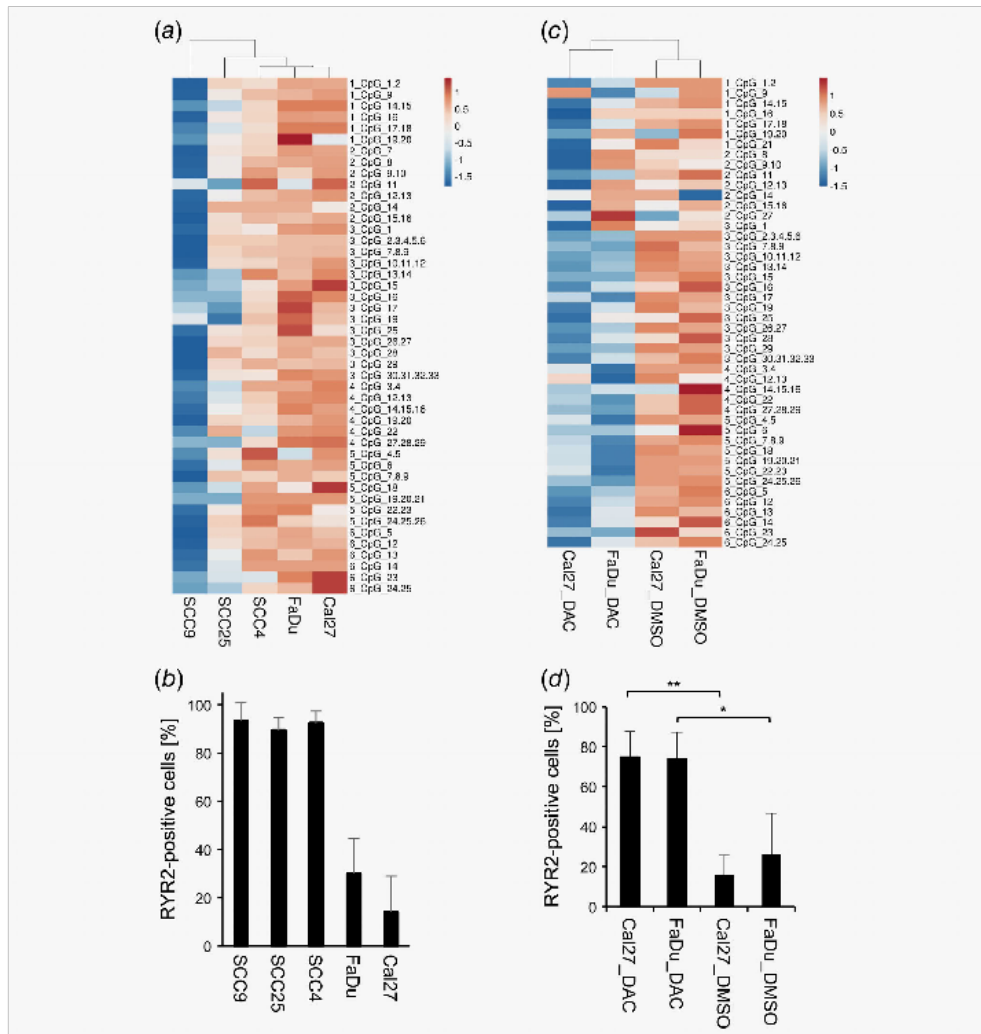


**Figure 3.** RYR2 promoter methylation and protein expression in HNSCC cell lines. Heatmaps were generated by unsupervised hierarchical clustering of MassARRAY data for CpGs (rows) applying Euclidean distance and average linkage on columns (HNSCC cell lines) and show differences in RYR2 promoter methylation for HNSCC cell lines under normal growth conditions (a) and upon treatment with Decitabine (DAC) or DMSO as control (c). (b) and (d) Graphs show the percentage of RYR2-positive cells as determined by FACS-aided quantification of five independent fields per cell lines and treatment. Bars represent mean values  $\pm$  SD of three independent experiments. Unpaired t test: \* $p$  value  $<0.05$  and \*\* $p$  value  $<0.001$ . [Color figure can be viewed at [wileyonlinelibrary.com](http://wileyonlinelibrary.com)]

We addressed whether variable RYR2 promoter methylation and expression also occur in HNSCC cell lines *in vitro*. Genomic DNA from five well-established HNSCC cell lines was evaluated by MassARRAY analysis and RYR2 promoter methylation was related to protein expression as determined

by IIF staining (Figs. 3a and 3b, Supporting Information Fig. S6A). HNSCC cell lines with low to moderate gene promoter methylation (SCC4, SCC9 and SCC25) showed a prominent and perinuclear RYR2 staining pattern in almost all cells, while only a subpopulation of RYR2-positive cells was detected

for those cell lines with gene promoter hypermethylation (FaDu and Cal27). These data suggested a regulation of RYR2 expression by gene promoter methylation in established HNSCC cell lines. Indeed, treatment of FaDu and Cal27 cells with the DNMT-inhibitor DAC increased RYR2 transcript levels and the amount of RYR2-positive cells as compared to DMSO-treated controls (Fig. 3d, Supporting Information Figs. S6B and S6C). DAC-induced RYR2 expression was accompanied by demethylation of CpGs in the proximal RYR2 promoter as determined by MassARRAY analysis (Fig. 3c).

#### RYR2-related $Ca^{2+}$ release

RYR2 is a major component of the intracellular  $Ca^{2+}$  release pathway in cardiomyocytes but is also expressed in nonexcitable cells. To demonstrate RYR2 function in HNSCC cell lines, SCC4 cells with prominent basal RYR2 expression were preloaded with the  $Ca^{2+}$  sensitive fluorophore Fluo 4 and subsequently stimulated with the potent RYR2 agonist Caffeine.<sup>30</sup> Single cell imaging revealed that SCC4 cells exhibit no  $Ca^{2+}$  release under control conditions, while  $Ca^{2+}$  peaks were detected after Caffeine administration (Supporting Information Figs. S6D and S6E). It is worth noting that the relative amount of SCC4 cells with Caffeine-induced  $Ca^{2+}$  release events (86%) coincided with the amount of RYR2-positive cells as determined previously by IF analysis (Fig. 3b). Moreover, Caffeine-induced  $Ca^{2+}$  release was abolished in most of the analyzed SCC1 cells (98%) upon preincubation with the selective RYR2 inhibitor Ryanodine (Supporting Information Fig. S6F). These data provided compelling experimental evidence that RYR2 is not only expressed but also functions as  $Ca^{2+}$  release channel in established HNSCC cell lines.

#### Loss of RYR2 protein expression during malignant progression

We addressed the question of whether silencing of RYR2 expression becomes evident at a specific time point during HNSCC pathogenesis. FFPE samples of the HLP0-HNC cohort ( $n = 9$ ) and a cohort of oral cancer patients from Brazil (UFRCIS,  $n = 7$ ) that shared areas of malignant tumor as well as adjacent normal and dysplastic mucosae were selected for IHC staining. IHC staining confirmed a positive RYR2 expression in most keratinocytes of adjacent tissue, while areas of malignant tumors exhibited a more heterogeneous staining pattern ranging from prominent staining in almost all tumor cells to a complete loss of staining (Fig. 4a). Most samples also showed a strong staining for stromal cells in the tumor microenvironment most likely representing infiltrating immune cells.

Quantification of the relative amount of RYR2-positive normal and dysplastic keratinocytes or cancer cells, respectively, indicated a gradual decrease of RYR2 expression with dysplasia and an even further reduction in malignant tumors as compared to normal mucosa or dysplastic lesions (Fig. 4b). Reduced RYR2 expression in invasive tumors as compared to adjacent dysplastic tissue was further confirmed with matched samples from

independent cases of the HLP0-HNC cohort ( $n = 10$ ), for which no normal mucosa but dysplastic areas were detectable (Fig. 4c). In addition, tissue sections from an independent cohort with nonmalignant lesions were analyzed by IHC staining and revealed a RYR2 expression pattern which was similar to adjacent dysplastic tissue of HNSCC (mean score  $2.52 \pm 0.88$ ,  $n = 26$ ). Finally, we identified serial FFPE specimens from two patients, who progressed from a nonmalignant dysplastic lesion to HNSCC over a time period of up to 5 years. Representative pictures of an IHC staining of these samples support a gradual loss of RYR2 expression during malignant progression (Supporting Information Fig. S7).

Although the amount of cases was limited ( $n = 19$ ), it is worth noting that patients with a reduced RYR2 expression score at the adjacent tissue had a significantly reduced progression-free survival as compared to their counterparts with a normal mucosa like score (Fig. 4d).

#### Discussion

In our study, we conducted a step-wise approach and unraveled RYR2 as a candidate gene with a high frequency of somatic mutations and promoter hypermethylation in samples from primary HNC patients. RYR2 is a major component of the intracellular  $Ca^{2+}$  release pathway and is associated with the sarcoplasmic or endoplasmic reticulum of several cell types, particularly in cardiomyocytes.<sup>55,57</sup> In cardiomyocytes, RYR2-mediated  $Ca^{2+}$  release is crucial for excitation-contraction coupling and mutations in RYR2 are associated with fatal cardiac arrhythmias and heart failure.<sup>51–53</sup> However, the functional role of RYR2 in nonexcitable cells under physiological and pathological conditions remains controversial.

Although a high RYR2 mutation frequency is a common feature of numerous human malignancies (Supporting Information Fig. S3C), the relevance of RYR2 in the pathogenesis of cancer has been questioned on the basis of its genomic properties as well as predominant expression and function in cardiomyocytes.<sup>17</sup> Our data indicate that silencing of RYR2 transcription by gene promoter methylation is a common event during HNSCC pathogenesis, but also other human cancers. However, in a substantial amount of cases somatic mutations occur and two findings support the assumption that cancer-related somatic mutations might affect RYR2 protein function: (i) coding nonsynonymous SNVs, which were found in the TCGA HNC and HLP0-HNC cohorts, were analyzed with well-established algorithms (MutationAssessor, MutationTaster, PolyPhen 2, CADD, SIFT and FATHMM) to predict a functional consequence of missense variations. For more than two thirds of detected missense variations, a damaging or disease-causing consequence with an impact on protein function was predicted by at least 75% of these algorithms (Supporting Information Table S7), and (ii) 10 HNC-linked missense variants are also listed in public databases (<https://www.ncbi.nlm.nih.gov/clinvar/> and <https://databases.lovd.nl/shared/genes/RYR2>) and are related to catecholaminergic polymorphic ventricular tachycardia, cardiac

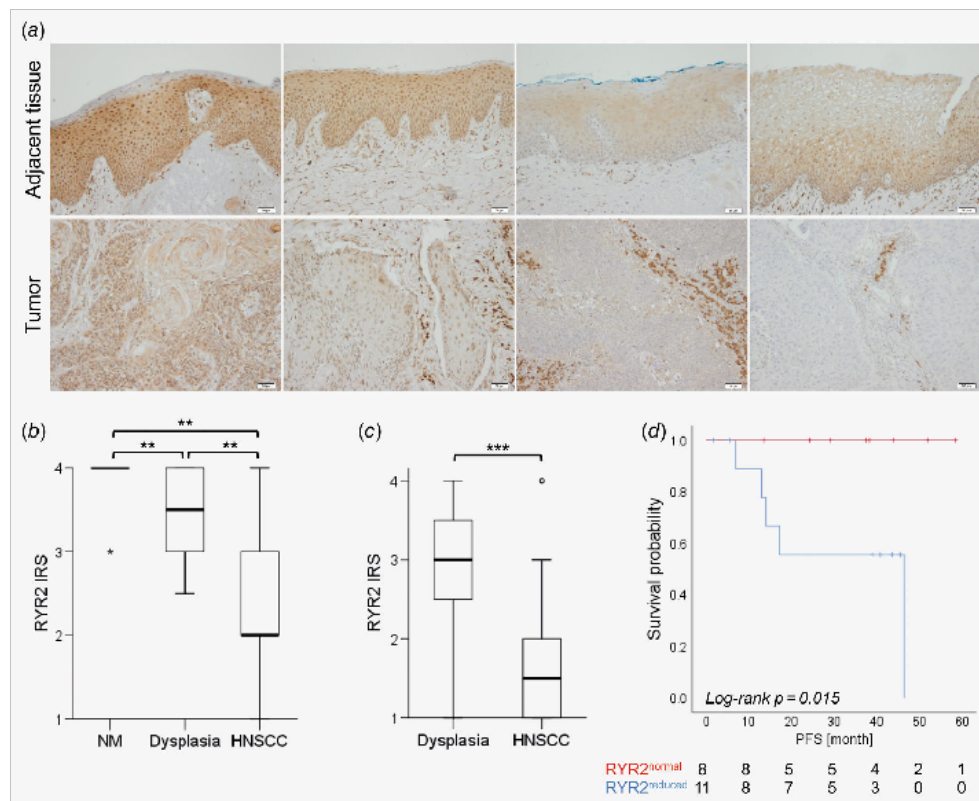


**Figure 4.** RYR2 expression in normal, dysplastic and malignant tissues. (a) Representative pictures of an IHC staining with FFPE tissue sections demonstrate RYR2 expression patterns (brown signal) in adjacent tissue (upper panel) and matched malignant tumor tissue (lower panel) of selected samples from the HIPO-HNC cohort. Box plots summarize the distribution of the RYR2 immunoreactivity score (IRS) as determined by IHC staining of tissue sections from the HIPO-HNC ( $n = 9$ ) and UFRGS ( $n = 7$ ) cohorts with matched areas of normal mucosa, dysplasia and malignant tumor (b) or tissue sections from independent cases of the HIPO-HNC ( $n = 10$ ) cohort and validation cohorts ( $n = 12$ , Ulm and Giessen) with matched areas of dysplasia and malignant tumor (c). The RYR2 IRS represents the relative amount of RYR2-positive keratinocytes or tumor cells from absent (1) to  $\geq 6\%$  (4). (d) Kaplan-Meier graph shows a significant difference in progression free survival (PFS) between subgroups of patients with normal (IRS = 4, red line) or reduced RYR2 expression (IRS < 4, blue line) in adjacent tissue. Numbers below the graph represent patients at risk at the indicated time points. Wilcoxon test: \*\* $p$ -value < 0.005, \*\*\* $p$ -value < 0.0005. [Color figure can be viewed at [wileyonlinelibrary.com](http://wileyonlinelibrary.com)]

arrhythmia or cardiovascular phenotype. For some of these missense variants, experimental data confirm their impact on RYR2 function. As an example, the missense mutation R176Q which is associated with arrhythmogenic right ventricular dysplasia type 2 causes structural alterations which are linked to channel dysfunction.<sup>53</sup> In a mouse knock-in model, the R176Q mutation predisposes the heart to catecholamine-induced oscillatory calcium-release events that trigger a calcium-dependent ventricular arrhythmia.<sup>54</sup>

Our data suggest a potential role of RYR2-dependent  $Ca^{2+}$  signaling in differentiation and tissue homeostasis, which

is supported by the fact that RYR2 was detected by Denda *et al.*<sup>55</sup> in epidermal keratinocytes with increased expression in differentiating as compared to proliferative keratinocytes *in vitro*.  $Ca^{2+}$  imaging after agonist and antagonist treatment indicated that RYR2 is not only expressed but also functional in a HNSCC cell line with prominent basal RYR2 expression as it is in epidermal keratinocytes.<sup>55</sup> Altered RYR2 activity either due to somatic mutation or epigenetic silencing might impair differentiation and thereby might accelerate malignant progression of transformed keratinocytes in combination with other oncogenic events. In line with this assumption, RYR2

promoter methylation is common in HPV-driven tumors, which are often characterized by a nonkeratinizing and basaloid histopathology as well as the absence of detectable premalignant dysplastic lesions.<sup>56</sup>

So far, only a few studies addressed RYR2 regulation and function in epithelial tumor cells. RYR2 expression and Caffeine-stimulated Ca<sup>2+</sup> release were reported for prostate and breast cancer cell lines.<sup>57,58</sup> Mariot *et al.*<sup>59</sup> provided experimental data that a RYR-related Ca<sup>2+</sup> mobilization augments apoptosis of LNCaP cells, a RYR1- and RYR2-positive prostate cancer cell line. In contrast, a strong RYR2 up-regulation was found in a breast cancer cell line upon EGF-induced epithelial-to-mesenchymal transition,<sup>58</sup> a process which is related with a higher risk for tumor cell dissemination and treatment failure in many epithelial malignancies, including HNSCC.<sup>60</sup> These controversial findings indicate a context-dependent function of RYR2 in epithelial and tumor cells derived thereof, and it will be a major challenge in future studies to unravel underlying molecular principles by loss of function and gain-of-function approaches.

IHC staining of tissue sections demonstrated a gradual loss of RYR2 protein expression from adjacent normal mucosa via dysplastic lesions to cancer, which is most likely due to an increase in promoter methylation. Our findings raise the attractive question, whether reduced RYR2 expression and/or an increase of promoter methylation in premalignant lesions of the head and neck region could serve as diagnostic biomarkers to assess the risk of malignant conversion and to facilitate timely and adequate treatment. This issue remains an unmet medical need of high clinical relevance,<sup>61</sup> but a large collection of premalignant tissue samples from patients with or without subsequent

diagnosis of HNSCC will be required to finally answer this question. Moreover, reduced RYR2 expression in adjacent tissue of primary HNSCC served as a risk factor for shorter progression-free survival. Low RYR2 expression may indicate the presence of altered keratinocyte differentiation due to genetic and/or epigenetic changes in the field surrounding the tumor. The concept of field cancerization, which is attributed to premalignant fields surrounding the primary tumor, has been shown to drive the high rate of local recurrence in HNSCC,<sup>62,63</sup> and molecular studies have provided compelling experimental evidence that the majority of HPV-negative HNSCC, but also other epithelial cancers, develop within local fields of premalignant cells that are clonally related to the resected primary cancer.<sup>64</sup> However, the samples size in our study was limited and the potential association between low RYR2 expression in tumor adjacent tissue and field cancerization or premalignant field requires further confirmation in a larger prospective study.

#### Acknowledgements

We are grateful to Marion Bähr, Oliver Mücke, Barbara Schwager, Claudia Birmüller, Anja Schumann and Nataly Henfling for excellent technical assistance, and thank Christina Görg, Bettina Messburger, Katrin Plütze (Center for Personalized Oncology (DKFZ HIPO), Heidelberg, Germany) as well as Melanie Bewerunge-Hudler and Angela Schulz (Core Facility Genomics & Proteomics, DKFZ Heidelberg, Germany) for providing excellent services. We thank the tissue bank of the National Center for Tumor Disease (Institute of Pathology, University Hospital Heidelberg, Germany) for providing paraffin embedded tumor specimens. This work was supported by the German Cancer Research Center-Heidelberg Center for Personalized Oncology (DKFZ HIPO), the NCT Precision Oncology Program (NCT POP), NCT 3.0\_2015.21 NCT-PRO, Coordination of Improvement of Higher Level Personnel (CAPIES) and the IMED-HNSCC Funding Program of the Helmholtz Initiative on Personalized Medicine.

#### References

- Forastier L, Sreerajkumar J, Dikshit R, et al. Cancer incidence and mortality worldwide: sources, methods and major patterns. *Lancet Glob Health* 2012; **10**:1-8.
- Leemans CR, Sjaloudis PJ, Brakenhoff RH. The molecular landscape of head and neck cancer. *Nat Rev Cancer* 2018; **18**:369-82.
- Castellano X, Alwan Y, Quer M, et al. HPV involvement in head and neck cancers: comprehensive assessment of biomarkers in 3680 patients. *J Natl Cancer Inst* 2018; **110**:e13003.
- Gillison ML, Chaturvedi AK, Anderson WF, et al. Epidemiology of human papillomavirus-positive head and neck squamous cell carcinoma. *J Clin Oncol* 2015; **33**:3783-90.
- Kikugawa T. Survivorship and quality of life in head and neck cancer. *J Clin Oncol* 2015; **33**:322-7.
- Chim MV, Myers EN. Oral cavity carcinoma: current management, controversies, and future directions. *J Clin Oncol* 2015; **33**:3669-76.
- Sacco AG, Cohen EE. Current treatment options for recurrent or metastatic head and neck squamous cell carcinoma. *J Clin Oncol* 2015; **33**:3309-11.
- Hellberg SL, Guá G, Chikova SL, et al. Genetic landscape of metastatic and recurrent head and neck squamous cell carcinoma. *J Clin Invest* 2016; **126**:169-80.
- Kang H, Kiess A, Chang CL. Emerging biomarkers in head and neck cancer in the era of genomics. *Nat Rev Clin Oncol* 2015; **12**:11-26.
- Agrawal N, Frederick MJ, Pickering CR, et al. Exome sequencing of head and neck squamous cell carcinoma reveals activating mutations in NOTCH1. *Science* 2011; **333**:1153-7.
- Strawhecker N, Aguiar AM, Tward AD, et al. The mutational landscape of head and neck squamous cell carcinoma. *Science* 2011; **333**:1157-60.
- Cancer Genome Atlas Network. Comprehensive genomic characterization of head and neck squamous cell carcinomas. *Nature* 2015; **522**:307-32.
- Kock MK, Zuo Z, Khattar A, et al. Integrative analysis of head and neck cancer identifies two biologically distinct HPV and three non-HPV subtypes. *Clin Cancer Res* 2015; **21**:670-81.
- Weichmann G, Rusidowski M, Krahn S, et al. The role of HPV RNA transcription, immune response, and telomerase expression and disruption TP53 mutations in diagnostic and prognostic profiling of head and neck cancer. *Int J Cancer* 2018; **172**:848-57.
- Länge A, Leck S, Gudziel V, et al. Low cancer stem cell marker expression and low hypoxia identify good prognosis subgroups in HPV(-) HNSCC after postoperative radiochemotherapy: a multicenter study of the DKKX-ROG. *Clin Cancer Res* 2016; **22**:3689-93.
- Lawrence NS, Stojanov P, Polak P, et al. Mutational heterogeneity in cancer and the search for new cancer-associated genes. *Nature* 2013; **499**:211-8.
- Hannemann PS, Hayes DN, Granda TR. Therapeutic insights from genomic studies of head and neck squamous cell carcinomas. *Cancer Discov* 2015; **5**:259-71.
- Krüger J, Sierra S, Hess J. Predictive value of epigenetic alterations in head and neck squamous cell carcinoma. *Mol Cell Oncol* 2014; **1**:e1027.
- Hans BA, Smith RV, Adkins LC, et al. Diverse DNA methylation loci distinguish anatomical site and HPV status in head and neck squamous cell carcinoma. *Clin Cancer Res* 2013; **19**:344-55.
- Dronman K, Koenig L, Gentles AJ, et al. Identification of an epigenetic head and neck squamous carcinoma subtype featuring the CpG Island methylator phenotype. *EBioMedicine* 2017; **17**:33-36.
- Rodríguez Perodes N, Esteller M. Cancer epigenetics reaches mainstream oncology. *Nat Rev Clin Oncol* 2014; **10**:7550-9.

22. Gnanapavan R, Michalidis C, Mandouris I, et al. Key tumor suppressor genes inactivated by 'greater promoter' methylation and serine mutations in head and neck cancer. *Epigenetics* 2014;9:1631-46.
23. Escribano J, Spencer C, Miyashiro K, et al. Complementary DNA synthesis in situ methods and applications. *Methods Mol Biol* 1882:218-66. 190.
24. Ritchie ME, Phipps R, Wu D, et al. Limma powers differential expression analyses for RNA sequencing and microarray studies. *Nucleic Acids Res* 2015;43:e77.
25. Shi W, Oshlack A, Smyth GK. Optimizing line noise versus bias trade-off for Illumina whole genome expression. *Bioinformatics* 2010;26:2734-40.
26. Arcey MJ, Iaffi AE, Corrado-Dravo H, et al. Minfi: a flexible and comprehensive bioconductor package for the analysis of Illumina DNA methylation microarrays. *Bioinformatics* 2014;30:1363-9.
27. Triche TJ Jr, Weisenberger DJ, Van Den Berg D, et al. Low level processing of Illumina Infinium DNA methylation BeadArrays. *Nucleic Acids Res* 2013;41:e99.
28. Boutin TP, Triche TJ Jr, Hansen KD. Preprocessing, normalization and integration of the Illumina HumanMethylationEPIC array with minfi. *Bioinformatics* 2017;33:581-82.
29. Fortin JP, Labbe A, Lemire M, et al. Functional normalization of 50K methylation array data improves replication in large cancer studies. *Genome Biol* 2014;15:e63.
30. R Studio Team. RStudio: Integrated Development for R. Boston, MA: Available from <http://www.rstudio.com/>; 2015. 7015.
31. Ehrlich M, Nelson MR, Sausville P, et al. Quantitative high-throughput analysis of DNA methylation patterns by base-specific cleavage and mass spectrometry. *Proc Natl Acad Sci USA* 2005;102:18745-50.
32. Abramov I, Vito J. Cytosine web tool for visualizing clustering of multivariate data using principal component analysis and heatmap. *Nucleic Acids Res* 2015;43:W566-70.
33. Hakee G, Hozeniger D, Schmitz M, et al. Biological evidence for a causal role of HPV16 in a small fraction of laryngeal squamous cell carcinoma. *Br J Cancer* 2013;109:73-83.
34. Deng G, Yang J, Zhang Q, et al. MethCNAC: a database for integrating genomic and epigenomic data in human cancer. *BMC Genomics* 2018;19:138.
35. Taxy B, Schwager C, Doffna O, et al. Comparative analysis of transcriptomic-based hypoxia signatures in head and neck squamous cell carcinoma. *Molecular Oncol* 2016;118:750-8.
36. Love MI, Huber W, Anders S. Moderated estimation of fold change and dispersion for RNA-seq data with DESeq2. *Genome Biol* 2014;15:550.
37. Schneider CA, Rasband WS, Licoeri KW. NIH Image to ImageJ: 25 years of image analysis. *Nat Methods* 2012;9:671-5.
38. Jones DT, Hutter B, Jager N, et al. Recurrent somatic alterations of *CCNE1* and *NCRA2* in pituitary astrocytomas. *Acta Otolaryng* 2017;145:927-32.
39. Jones DT, Jager N, Koul M, et al. Dissecting the genomic complexity underlying medulloblastoma. *Nature* 2012;488:100-5.
40. Stan JD, Karpman BM, Campbell P, et al. Data analysis to create a cloud commons. *Nature* 2015; 523:149-51.
41. Wang L, Li M, Hakonarson H. ANNOVAR: functional annotation of genetic variants from high-throughput sequencing data. *Nucleic Acids Res* 2010;38:e164.
42. Ramirez A, Pflanz H, Madsen T, et al. Integrating mapping, assembly, and haplotype-based approaches for calling variants in clinical sequencing applications. *Nat Genet* 2014;46:912-8.
43. Reva B, Antipin Y, Sander C. Predicting the functional impact of protein mutations: application to cancer genomics. *Nucleic Acids Res* 2011;39:e118.
44. Schwarz M, Cooper DN, Schmeike M, et al. MutationCaster: mutation prioritization for the deep sequencing age. *Nat Methods* 2014;11:351-7.
45. Adahubei OA, Schriek S, Posheln I, et al. A method and server for predicting damaging missense mutations. *Nat Methods* 2010;7:218-9.
46. Reznick Z, Wilton D, Cooper GM, et al. CADD: predicting the deleteriousness of variants throughout the human genome. *Nucleic Acids Res* 2019; 47:D886-D894.
47. Sim NL, Kumar P, Liu J, et al. SIFT web server: predicting effects of amino acid substitutions on proteins. *Nucleic Acids Res* 2012;40:W412-7.
48. Shihab HA, Rogers MF, Ghosh J, et al. An integrative approach to predicting the functional effects of non-coding and coding sequence variation. *Bioinformatics* 2015;31:1536-43.
49. Shihab JA, Gough J, Cooper DN, et al. Predicting the functional, molecular, and phenotypic consequences of amino acid substitutions using hidden Markov models. *Bioinformatics* 2013;29:57-65.
50. Van Peltgers D. Ryanodine receptor 2 loss erases ion channel giants. *J Biol Chem* 2015;497:21-53.
51. Lauerer HJ, Georgiev DK, Ischi AD, et al. Ryanodine receptors: structure, expression, molecular details and function in calcium release. *Cold Spring Harb Perspect Mol Biol* 2016;2:a019566.
52. Chen W, Wang R, Chen B, et al. The ryanodine receptor channel sensing gate controls Ca<sup>2+</sup> waves and Ca<sup>2+</sup>-triggered arrhythmias. *Nat Med* 2011; 17:181-92.
53. Avadori P, Kirilovic I, Stethopoulos PR, et al. Type 2 ryanodine receptor domain contains a unique and dynamic alpha-helix that transitions to a beta-strand in a mutant linked with a heritable cardiomyopathy. *J Mol Biol* 2013;425:1031-46.
54. Kamenkovič J, Vrbil J, Gm, Gosevsek USA, et al. Mice with the R76Q cardiac ryanodine receptor mutation exhibit calcium-induced ventricular tachycardia and cardiomyopathy. *Proc Natl Acad Sci USA* 2006; 103:2179-84.
55. Danda S, Kurumoto T, Taki K, et al. Ryanodine receptors are expressed in epidermal keratinocytes and associated with keratinocyte differentiation and epidermal permeability barrier homeostasis. *J Invest Dermatol* 2012;132:69-75.
56. Chakravarthy A, Henderson S, Thirdborough SM, et al. Human capillarioides tumor development throughout the head and neck: improved prognosis is associated with an immune response largely restricted to the oropharynx. *J Clin Oncol* 2016;34:4132-41.
57. Kobayashi S, Gusterson B, Eickholt CD. Identification of ryanodine receptor isoforms in mouse DU-145, LNCaP, and PWR-1E cells. *Biochem Biophys Res Commun* 2012;425:431-5.
58. Davis PM, Persson M, Gallo PJ, et al. Assessment of gene expression of ion channels, pumps and exchangers with epidermal growth factor-induced epithelial-mesenchymal transition in a breast cancer cell line. *Cancer Cell Int* 2013;13:96.
59. Varin P, Preza-Skaya N, Rouilhac MM, et al. Evidence of functional ryanodine receptor involved in prognosis of prostate cancer (LNCaP) cells. *Prostate* 2000;43:205-14.
60. Thakout I, Veit JA, Hess J. Epithelial-to-mesenchymal transition in the pathogenesis and therapy of head and neck cancer. *Cancers (Basel)* 2017;9:176.
61. Nishimura HK, Saito T, Smith J, et al. Treatment and follow-up of oral dysplasia—a systematic review and meta-analysis. *Head Neck* 2009;31:600-9.
62. Ryszczyk MD, Lee WC, Ready NE, et al. Quantifying the dynamics of fluid canceration in nasopharyngeal head and neck cancer: a multi-scale modeling approach. *Cancer Res* 2016;76:7078-88.
63. Ikenoue CR, Dugalis BJ, Brakenhoff RH. The molecular biology of head and neck cancer. *Nat Rev Cancer* 2011;11:19-22.
64. Tabo M, Brakenhoff RH, van Houten VM, et al. Persistence of genetically altered fields in head and neck cancer patients: biological and clinical implications. *Clin Cancer Res* 2001;7:523-37.





DKFZ  
 Prof. Dr. Karin Hoppe-Seyler  
 F065 Mol. Ther. virusassoz. Tumore  
 Im Neuenheimer Feld 280  
 69120

Multiplexion GmbH  
 Virchowstr. 51  
 88048 Friedrichshafen  
 Fon: +49 (0) 7545 7759044  
 E-Mail: info@multiplexion.de  
 www.multiplexion.com

## Human Cell Line Authentication Report

Report ID	1549	Order ID	1627
Report Date	11.08.2016	Order Date	21.07.2016
		Purchase No.	45516407

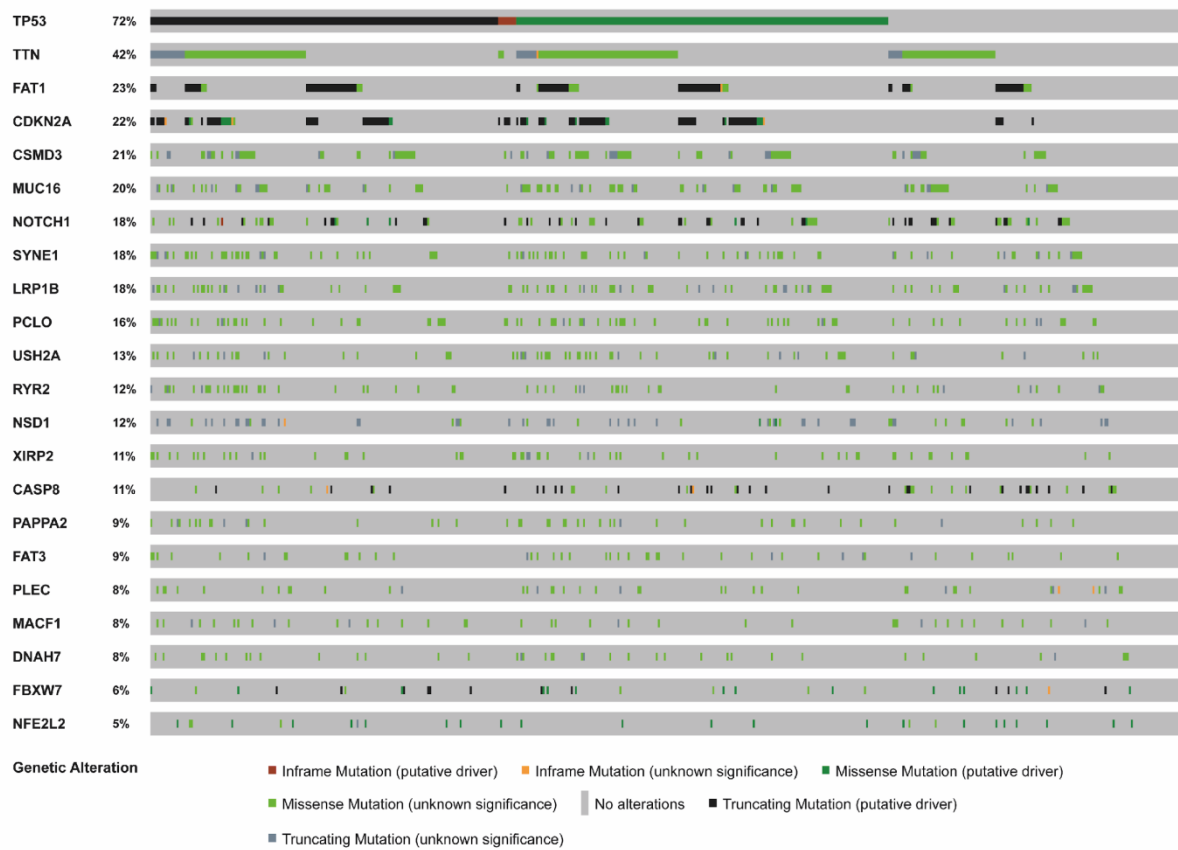
Dear Prof. Dr. Karin Hoppe-Seyler,  
 Many thanks for your order. The Multiplex human Cell line Authentication Test (MCA) was performed as described at [www.multiplexion.de](http://www.multiplexion.de). Please find below the results.  
 Best regards,  
 Dr. Markus Schmitt

Information from Customer				Results			Summary			
Sample ID	Sample Name	Cell line name	If other: exact name	DNA quality	Best Hit with DataBase	Identity (%)	Present in Database?	Cross-Contamination?	Identity confirmed?	Genotype Code
2971	FaDu	FaDu		ok	FaDu	98	yes	no	confirmed	AATTAAAAATTAATTTAATTAATAATTA AAAAAAAATTAATAAAAT
2972	Cal27	CAL-27		ok	CAL-27	100	yes	no	confirmed	AWTTTAAATAAATAATAATAAAWTTTTT AAAAAATAATTAATTTTA
2973	SCC4	SCC-4		ok	SCC-4	98	yes	no	confirmed	AATTATAAATAATAATAATAATTTTA AAAAAATAATAWTTTTTAT
2974	SCC25	SCC-25		ok	SCC-25	98	yes	no	confirmed	AWTTTAAATTTAAATAAATAATAATTNN NNAAAAATAATTTTAAAAAT
2975	SCC9	SCC-9		ok	SCC-9	98	yes	no	confirmed	ATTTATAATAAATAATAATAATTTAAT TAATTWTTTAAATTTTAT

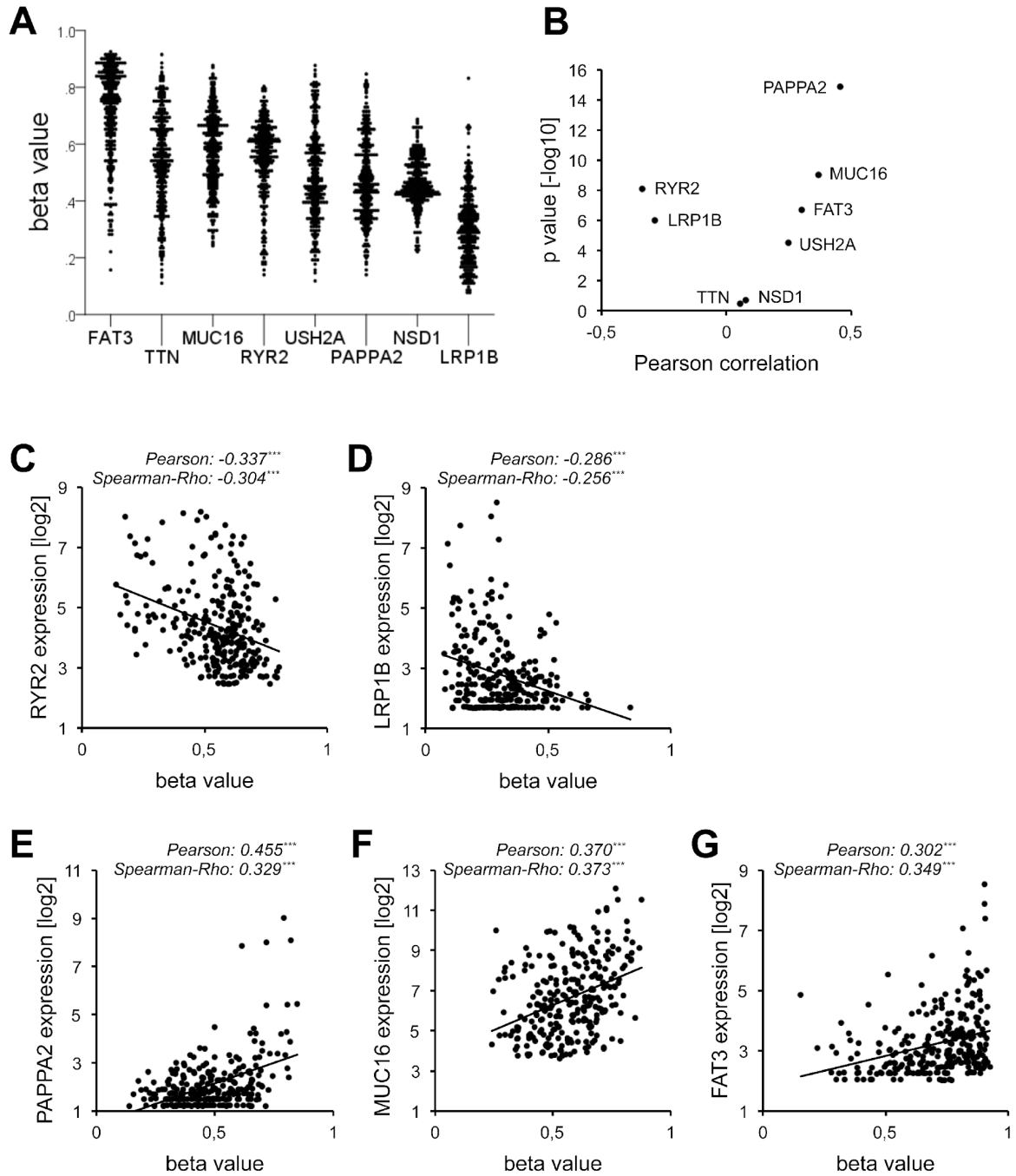
### Legend:

DNA quality:	ok, good DNA quality detected; invalid, DNA was absent or degraded or from non-human species
Identity (%)	Identity of submitted cell line to best hit of data base; identical: 98% and above, not identical: <96. Please note, a 96% or 98% identity may hint at loss of heterozygosity, which might be due to overlong passaging.
Present in data base?	indicates whether submitted cell line is included in MCA data base. If not included, then no identity confirmation can be made.
Cross-contamination?	indicates whether detected cell line is cross-contaminated by additional cells from another human cell line, the contaminating cell line cannot be specifically identified
Identity confirmed?	"confirmed", identity was confirmed by MCA (>95%); "false", submitted cell line shows a cross-match with a cell line present in data base; "unique sequence", cell line is not present in data base and shows a genotype code that is not related to any cell line included in the data base (<95%)
Genotype Code	48-letter code for 24 SNP locations; W, uncertain signal; N, no call

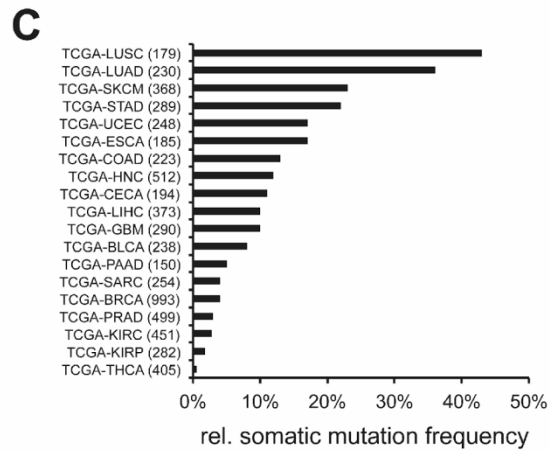
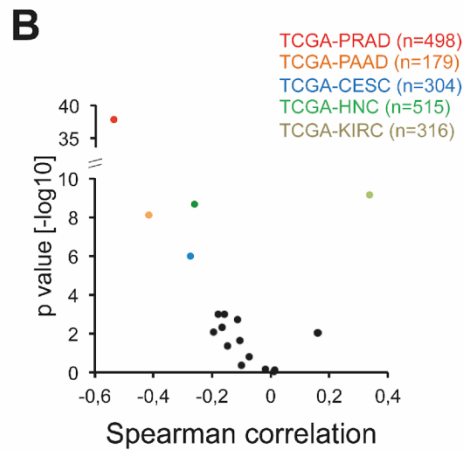
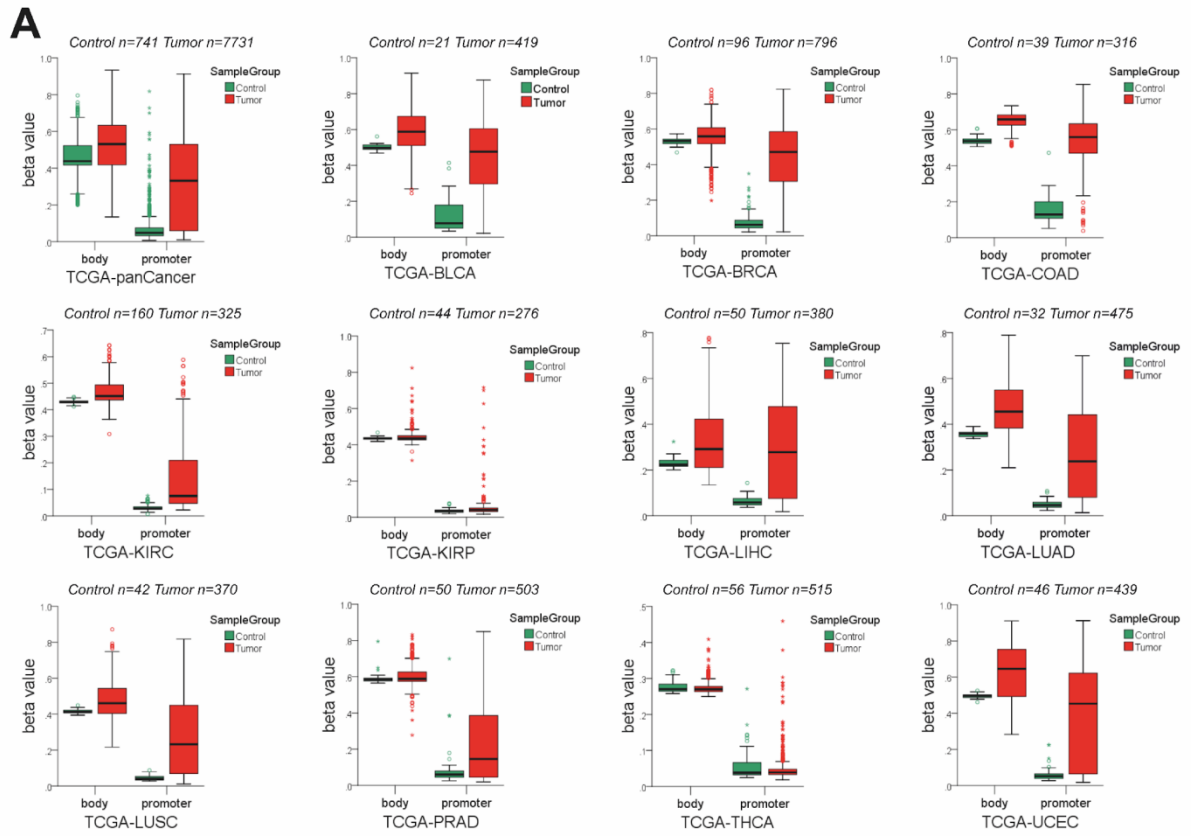
Multiplexion GmbH  
 CEO: Dr. Markus Schmitt Company Register: Ulm HRB 730824  
 USt-Ident-No. DE283400605



*Schmitt et al., Supplemental Figure S1*



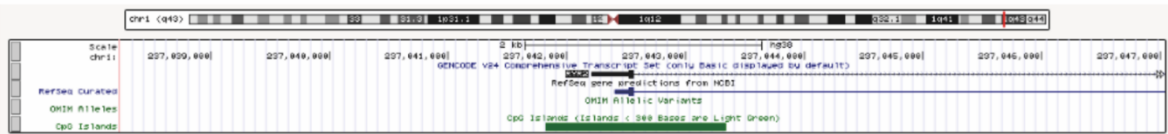
Schmitt et al., Supplemental Figure S2



Schmitt et al., Supplemental Figure S3

**A**

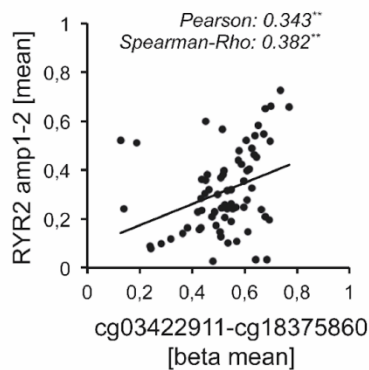
UCSC Genome Browser on Human Dec. 2013 (GRCh38/hg38) Assembly



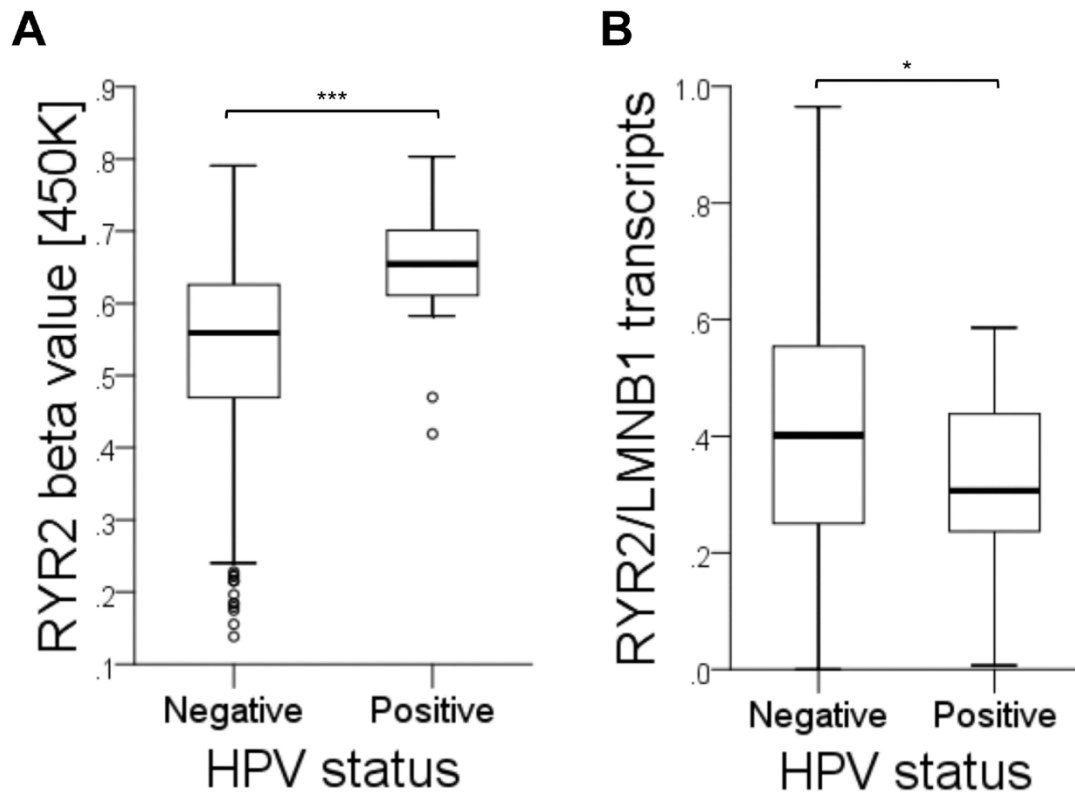
RYR2amp1, RYR2amp2,  
 RYR2amp3, RYR2amp4,  
 RYR2amp5, RYR2amp6

&gt;chr1:237041827-237043418

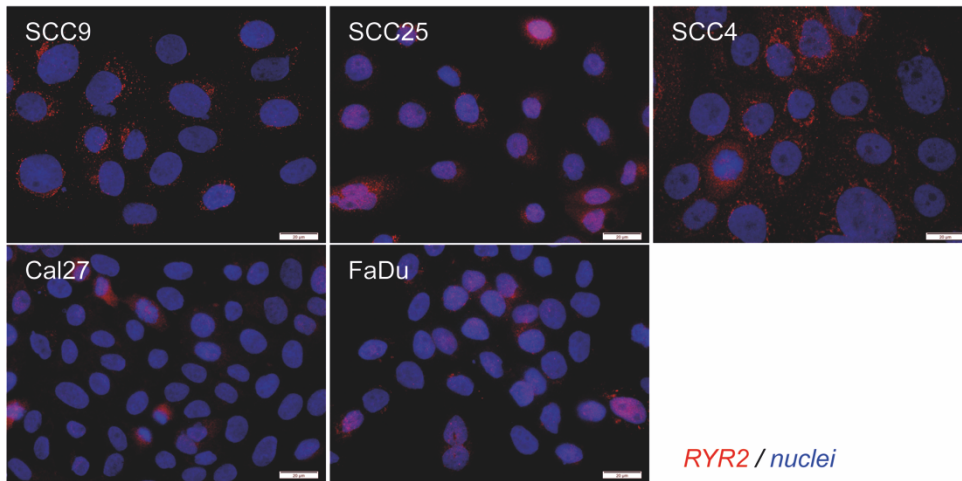
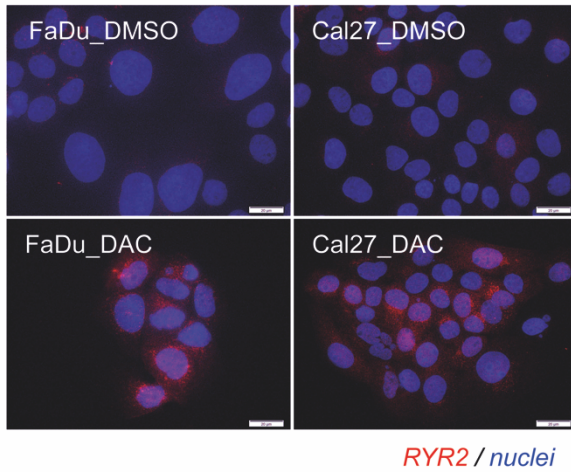
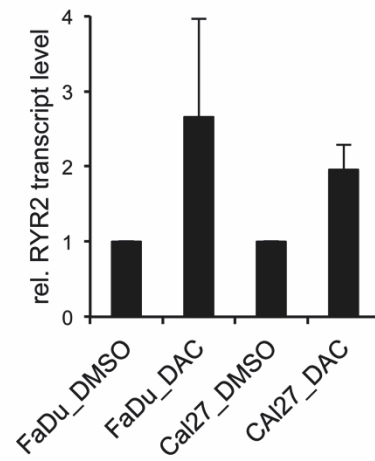
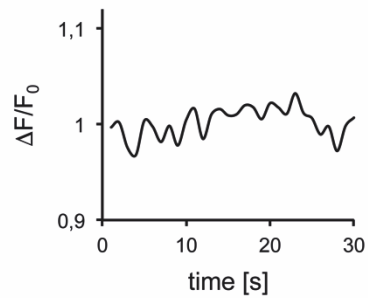
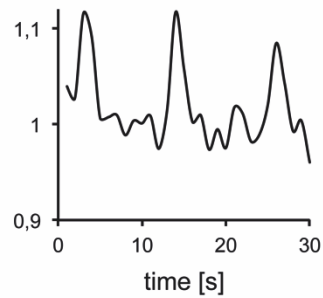
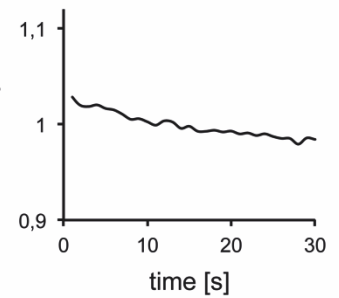
CGTGC GCCCAGGTGAAAGATATCATTTCTCCGTGCGAATCCGAAGTCCGTGGAAGTTAGTGCCCTAGCCAGTCCAGGAGGAAGGGGCGTCGTGCCG  
 ← cg19764418  
 CGGGTTTTAAGCTCGGAAGGGCAGGGGAATGAGCCAGGGACCCAGCGGGGCGCAGGTAGGAGCTGTGCGCTCGCCGGGTGCGCTCGGCCCCG  
 cg03422911  
 ATTCAGCGCAGCCAGTAAGTGGCGCTGGGCCTCGGGTTTGGCGGCCGGAGGAGCGGGCTCGGATTACCTGCAGCAGCGGGGAGCCGCCAGCT  
 CCTCCCGCCCGCCCCACACCCACCCACCGCTGCACTAACCCCGGCTCAGCTGGCTCCGCGCATTGCTCGGAGGAGCCGGGGCCGAGCGGAC  
 cg18375860  
 CGCCGGCTGCAGGCAGCGAGCGCGGCTGGGCTGCGGGGCTGCTCCCGCGTCTCCGGGCCCCGGGCCGCCCTCCTCCCGCACAGTGCGGAGCAGGG  
 AGGCCCGCGCCTCGACCACCCCGCCGAGCGTCCGCGCCTCCTCCTCCGCTCTGCAGGCGGGACCGCCCGCGCTCGGCACCCGGCAGCGCGCC  
 CCCCTCCAGCCCCCGGCTCCCGCAGCAGAAGCAGAAGGCAGCGCCAGGGGCGCCGCGCCCGCGAGCTCCGCGGGGCTCGGGAGCCGCCCGCGC  
 GAGGAGCGCGGAACCATGGCCGATGGGGGCGAGGGCGAAGACGAGATCCAGTTCTCGCAACTGTAAGCGCCGTGCGTGCCTGTGTCAGGGG  
 AAGGGGGCTCAGGGCATCCACTAGCGGGTCCGGCCAGAGTGACAGCGGGCAGCGGGACTCGCGGGCGGGGCGAGGGGGTGCCCTGAGGATGC  
 GGGAGGAGCGGGCATCACCAAGTGTGTGCAGGTGTGCGTGTGGGGCGAGGGAAGCAAGGCGCGTGTCTGTGCGCGCGTGTGGAAGCTAGAGGA  
 TGGAGCGCGGCTAGCCGGCGGCAGGCGCCCGGGCTCGGACCGGGCACCGGGGACAGGAGCGTCCGAGCTCGGGAAACCGGGAGAGGAGGGGACGG  
 CCGGTCCGGCTGCTTGGTGGCACCGCTGGGACTCCCGGGCGCCCGGGGCGAGGTCAGAGCAGGGTGGCCCGTGGGGGCGCGGGGAGCGCGGG  
 AACTCGGGCTGTTTCTGGGAATACCGCCCGCGGGAGGTTTCTTGGGCTTTCCGGCTGGACCGCGCGTTGTACCGGAGCGAAGACGTTGGTTCCGCTT  
 ACTCCGTGTAGCGTGCAGCAGCTGACCGGGGCGGGGTGATGTTGAGGACCGTCCGCGGAGGTTCCCCCAAGTCAAGGTGCTCGGAAGCGG  
 AGGAGGAGTCCCTCCGTTGTTCCCGCGGTTCCCGGGGCTGGTGCATCCGTGGTGGTGTGTGACCGCTTGCAAAGCGTGAAGGCATGGGAAGCG  
 AGCGTGTGTTTTCGTGTGTGCGCGCGCGGGTGGTGGTGGGGAGAACATCGTGAACGTTGTCTCTCAAATGCTGGCTTATTGCATGCCAAGTGA  
 AGCAAAGTGTGTGTGTGTAAGTGAAGGGCAGGGTGGCTG

**B**

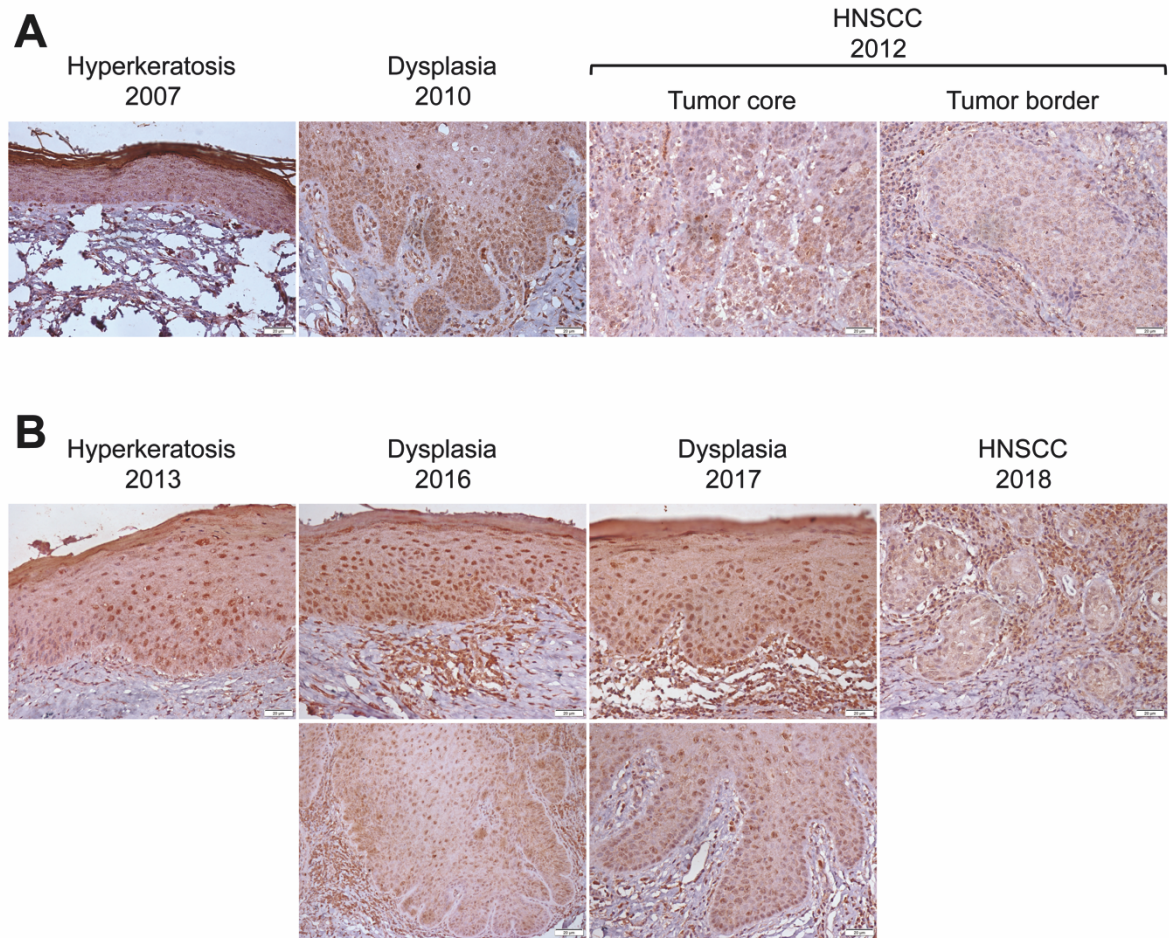
Schmitt et al., Supplemental Figure S4



*Schmitt et al., Supplemental Figure S5*

**A****B****C****D****E****F**

*Schmitt et al., Supplemental Figure S6*



*Schmitt et al., Supplemental Figure S7*



**Supplemental Table S1. Summary of clinical and histopathological features of the HIPO-HNC cohort**

Sample ID	WES	Methylome	MA	IHC RYR2	Subsite	Gender	Age [years]
HNC1	yes	yes	yes		oropharynx	male	60,69
HNC2	yes	yes	yes		oropharynx	female	57,48
HNC3	yes	yes	yes		oropharynx	male	61,44
HNC4	yes	yes	yes	yes	oropharynx	male	62,04
HNC5		yes	yes	yes	oropharynx	male	81,90
HNC6	yes	yes	yes		oropharynx	male	64,66
HNC7	yes	yes			oropharynx	male	48,21
HNC8	yes	yes			oropharynx	female	62,99
HNC9	yes	yes		yes	nasal cavity	male	45,84
HNC10	yes	yes	yes	yes	oropharynx	male	54,79
HNC11	yes	yes	yes		oropharynx	male	64,52
HNC12	yes	yes	yes		hypopharynx	male	65,24
HNC13	yes	yes			oropharynx	male	66,25
HNC14	yes	yes		yes	nasal cavity	male	66,07
HNC15	yes	yes	yes		oropharynx	male	52,88
HNC16	yes	yes	yes		oropharynx	male	56,51
HNC17	yes	yes	yes	yes	nasal cavity	male	75,30
HNC18	yes	yes	yes		larynx	male	61,99
HNC19	yes	yes	yes		nasal cavity	male	67,64
HNC20	yes	yes	yes		oral cavity	male	59,88
HNC21	yes	yes	yes		larynx	male	53,90
HNC22	yes	yes	yes	yes	oropharynx	male	54,59
HNC23	yes	yes	yes		larynx	male	66,21
HNC24	yes	yes			oral cavity	female	76,27
HNC25	yes	yes	yes		oral cavity	male	72,43
HNC26	yes	yes	yes		nasal cavity	male	45,82
HNC27	yes	yes	yes		oropharynx	male	63,62
HNC28	yes	yes		yes	oropharynx	male	71,55
HNC29	yes	yes			oral cavity	male	56,02
HNC30		yes		yes	oral cavity	male	55,32
HNC31	yes	yes	yes		oropharynx	male	67,75
HNC32	yes	yes	yes		oropharynx	male	55,76
HNC33	yes	yes	yes	yes	oropharynx	female	46,27
HNC34	yes	yes	yes		oral cavity	female	73,39
HNC35	yes	yes	yes		oropharynx	male	40,61
HNC36	yes	yes	yes		oropharynx	male	50,33
HNC37	yes	yes	yes		larynx	male	64,47
HNC38	yes	yes	yes	yes	oropharynx	female	54,57
HNC39	yes	yes	yes		oropharynx	male	56,60
HNC40	yes	yes	yes		oral cavity	male	60,44
HNC41	yes	yes	yes	yes	hypopharynx	male	72,86
HNC42	yes	yes	yes		oropharynx	male	48,12
HNC43	yes	yes	yes		larynx	male	69,22
HNC44	yes	yes	yes		oropharynx	male	64,27
HNC45	yes	yes			oral cavity	female	75,26

Tobacco	Alcohol	HPV-related	T status	N status	ECE	Pathological grading	Therapy
no	yes	yes	1	1	yes	3	SRCT
no	no	yes	2	1	no	3	SRT
yes	yes	yes	2	2	yes	3	SRCT
no	yes	yes	2	2	yes	2	SRCT
no	no	yes	1	1	yes	3	SRT
yes	yes	yes	2	1	yes	3	SRCT
yes	no	yes	2	0		1	S
yes	yes	no	2	0		2	S
yes	yes	no	2	0		2	S
yes	yes	no	2	2b	yes	2	SRCT
no	no	yes	4b	2	yes	3	SRCT
yes	yes	no	3	2b	yes	2	SRCT
yes	no	yes	2	0		2	S
no	yes	no	2	0		2	S
yes	yes	yes	2	0		3	SRT
yes	yes	no	3	1	no	2	SRCT
no	no	no	1	1	no	2	S
yes	no	no	4a	2b	yes	2	SRCT
yes	no	no	4	0		2	SRT
yes	yes	no	2	2b	yes	2	SRCT
yes	yes	no	4	0		2	SRCT
yes	no	no	2	0		3	SRCT
yes	yes	no	3	0		2	SRT
yes	no	no	2	0		3	S
yes	no	no	4a	1	yes	2	SRCT
no	no	no	4a	0		2	S
yes	yes	no	3	2b	yes	3	SRCT
yes	yes	yes	2	0		2	S
no	no	no	4	2c	no	3	SRCT
yes	yes	no	2	2c	no	2	SRT
yes	yes	no	1	2c	yes	3	SRCT
no	no	no	4a	2a	no	2	SRCT
yes	no	no	1	1	no	2	SRT
no	no	no	4a	0		2	SRT
no	no	yes	2	1	yes	2	SRCT
yes	yes	yes	3	2	yes	3	SRCT
yes	no	no	3	2c	yes	2	SRCT
yes	yes	no	2	1	yes	2	SRCT
yes	no	yes	2	1	no	3	SRT
yes	yes	no	4a	0		2	SRT
yes	yes	yes	4a	2c	yes	2	SRT
no	no	yes	2	1	no	3	S
yes	yes	no	3	0		2	S
yes	yes	yes	2	1	yes	2	SRCT
no	yes	no	3	1	no	3	S

**R-Status**

---

0  
0  
1  
1  
0  
0  
0  
0  
0  
0  
1  
1  
0  
0  
0  
0  
0  
0  
1  
0  
0  
0  
0  
0  
0  
1  
0  
0  
0  
0  
0  
0  
0  
0  
0  
0  
0  
0  
0  
0  
0  
0  
0  
0  
0  
0  
0  
0  
0  
0  
0  
0  
0  
0  
0  
0  
0  
1

HNC46	yes	yes	yes		oral cavity	male	77,99
HNC47	yes	yes	yes		larynx	female	59,26
HNC48	yes	yes	yes		nasal cavity	male	55,70
HNC49	yes	yes	yes		oral cavity	male	57,21
HNC50	yes	yes	yes		oropharynx	male	46,86
HNC51	yes	yes	yes		larynx	male	59,07
HNC52	yes	yes	yes		oral cavity	female	67,68
HNC53	yes	yes	yes		nasal cavity	male	55,55
HNC54	yes	yes			nasal cavity	female	59,49
HNC55	yes	yes	yes		larynx	female	82,52
HNC56	yes	yes	yes		hypopharynx	male	68,44
HNC57	yes	yes	yes		oropharynx	male	56,94
HNC58	yes	yes	yes		oral cavity	male	73,68
HNC59	yes	yes	yes	yes	hypopharynx	male	59,59
HNC60	yes	yes	yes		oral cavity	female	68,06
HNC61	yes	yes	yes		oropharynx	male	61,46
HNC62	yes	yes	yes		larynx	male	63,52
HNC63	yes	yes	yes		oropharynx	female	56,65
HNC64	yes	yes	yes		larynx	male	60,88
HNC65	yes	yes	yes		larynx	male	61,75
HNC66	yes	yes	yes		oropharynx	female	72,35
HNC67	yes	yes	yes	yes	oropharynx	male	51,55
HNC68	yes	yes	yes		larynx	male	49,45
HNC69	yes	yes	yes	yes	oral cavity	male	74,59
HNC70	yes	yes	yes		oral cavity	male	63,29
HNC71	yes	yes	yes		oral cavity	male	39,68
HNC72	yes	yes	yes		oropharynx	male	62,53
HNC73	yes	yes	yes		oropharynx	male	57,12
HNC74	yes	yes			oral cavity	male	56,31
HNC75	yes	yes	yes	yes	larynx	male	50,78
HNC76	yes	yes			larynx	male	55,68
HNC77	yes	yes	yes		oral cavity	female	63,45
HNC78	yes	yes	yes	yes	oral cavity	male	70,08
HNC79	yes	yes			nasal cavity	male	58,01
HNC80	yes	yes	yes		oral cavity	female	52,00
HNC81	yes	yes	yes	yes	oral cavity	female	65,56
HNC82	yes	yes	yes		nasal cavity	male	75,95
HNC83	yes	yes	yes		oropharynx	male	56,84
HNC84	yes	yes	yes		nasal cavity	female	68,07
HNC85	yes	yes	yes		oropharynx	female	66,58
HNC86	yes	yes		yes	oropharynx	male	61,39
HNC87	yes	yes	yes		oral cavity	male	56,85

WES= whole-exome sequencing; MA=MassARRAY; IHC=immunohistochemistry, ECE=extracapsular extension  
non-HPV-related=DNA negative or DNA positive but RNA negative; HPV-related= DNA and RNA positive  
S=surgery; RT= adjuvant radiotherapy; RCT= adjuvant radiochemotherapy

no	no	no	4a	0		2	S
yes	yes	no	4a	2b	no	2	SRT
no	no	no	4a	0		2	S
yes	yes	no	4a	2c	yes	2	SRCT
no	no	yes	2	1	yes	2	SRT
yes	yes	no	4a	1	no	3	SRT
no	no	no	4a	0		3	S
yes	yes	no	2	1	no	3	SRT
no	yes	no	2	0		3	S
yes	no	no	3	0		2	S
yes	no	no	2	2c	yes	2	SRT
no	yes	yes	3	2	no	3	SRCT
yes	yes	no	3	0		3	S
yes	yes	no	2	0		2	S
no	no	no	4	0		2	SRT
yes	yes	no	3	2c	yes	2	SRCT
yes	no	yes	4a	0		2	SRT
yes	no	no	3	0		2	SRCT
yes	no	no	4a	2b	no	2	S
yes	no	no	4a	0		3	SRT
no	no	yes	3	2	yes	3	SRCT
yes	yes	yes	2	1	yes	3	SRCT
yes	yes	no	3	1	yes	2	SRCT
yes	no	no	2	2c	yes	3	SRT
yes	yes	no	4a	1	no	2	S
no	no	no	2	2b	yes	2	SRCT
yes	yes	no	3	2c	yes	2	SRCT
yes	yes	no	2	2b	no	3	SRT
yes	no	no	1	0		2	S
yes	yes	no	3	0		2	S
yes	no	no	4a	0		3	SRT
yes	no	no	1	2b	no	3	SRT
yes	yes	no	4a	0		2	SRT
no	no	no	2	0		2	S
yes	no	no	4a	0		2	S
no	yes	no	2	2b	yes	2	SRCT
yes	no	no	4a	0		3	SRCT
yes	yes	yes	3	0		3	SRT
no	no	yes	4	0		2	SRT
yes	no	no	1	2b	yes	2	SRT
no	yes	yes	2	0		3	S
yes	yes	no	4a	3	yes	2	S

0  
1  
0  
0  
0  
0  
0  
0  
0  
0  
0  
0  
1  
1  
0  
0  
0  
0  
0  
0  
0  
0  
0  
0  
0  
0  
0  
0  
0  
0  
0  
1  
0  
0  
0  
0  
0  
0  
0  
0  
0  
0  
0  
0  
0  
1  
0  
1  
1  
1  
0  
1

---

**Supplemental Table S2. Histopathological features of the validation cohort (Ulm/Giessen/UFRGS)**

Sample ID	Subside	Diagnose	Normal mucosa
Giessen_1	larynx	leukoplakia	
Giessen_2	hypopharynx	CIS	
Giessen_3	oral cavity	CIS	
Giessen_4	oral cavity	CIS	
Giessen_5	larynx	CIS	
Giessen_6	oropharynx	CIS	
Giessen_7	larynx	dysplasia	
Giessen_8	larynx	dysplasia	
Giessen_9	larynx	dysplasia	
Giessen_10	larynx	dysplasia	
Giessen_11	oral cavity	CIS	
Giessen_12	larynx	CIS	
Giessen_13	larynx	dysplasia	
Giessen_14	larynx	dysplasia	
Giessen_15	larynx	dysplasia	
Giessen_16	larynx	SCC	
Giessen_17	larynx	SCC	
Giessen_18	larynx	CIS	
Giessen_19	larynx	dysplasia	
Giessen_20	larynx	papillomatous keratosis	
Giessen_21	larynx	SCC	
Giessen_22	larynx	dysplasia	
Giessen_23	larynx	leukoplakia	
Giessen_24	larynx	leukoplakia	
Giessen_25	larynx	leukoplakia	
Giessen_26	larynx	dysplasia	
Giessen_27	larynx	dysplasia	
Ulm_1	larynx	SCC	
Ulm_2	larynx	SCC	
Ulm_3	larynx	SCC	
Ulm_4	larynx	SCC	
Ulm_5	larynx	SCC	
Ulm_6	larynx	SCC	
Ulm_7	larynx	SCC	
Ulm_8	hypopharynx/larynx	SCC	
Ulm_9	pharynx	SCC	
Ulm_10	hypopharynx/larynx	SCC	
Ulm_11	larynx	SCC	yes
UFRGS_1		SCC	yes
UFRGS_2		SCC	yes
UFRGS_3		SCC	yes
UFRGS_4		SCC	yes
UFRGS_5		SCC	yes
UFRGS_6		SCC	yes
UFRGS_7		SCC	yes

*CIS=carcinoma in situ; SCC=squamous cell carcinoma*

<b>Dysplasia</b>	<b>Malignant tumor</b>
yes	
yes	
yes	
yes	
yes	
yes	
yes	
yes	
yes	
yes	
yes	
yes	
yes	
yes	
yes	
yes	
yes	
yes	
yes	
yes	yes
yes	
yes	
yes	
yes	
yes	
yes	yes
yes	yes
yes	yes
yes	yes
yes	yes
yes	yes
yes	yes
yes	yes
yes	yes
yes	yes
yes	yes
yes	yes
yes	yes
yes	yes
yes	yes
yes	yes
yes	yes
yes	yes
yes	yes
yes	yes
yes	yes
yes	yes



Supplementary Table S4 is available in: <https://onlinelibrary.wiley.com/doi/full/10.1002/ijc.32481>

**Supplemental Table S5. Summary of MassARRAY primers**

<b>Amplicon</b>	<b>Forward primer<sup>1</sup></b>	<b>Reverse primer<sup>2</sup></b>
RYR2amp1	GGGTAGGGGAATGAGTTTAGGG	CCAACTAAACCAAAATTAATACAAC
RYR2amp2	GGGTTGTGGATTATTTGTAGTAG	CACAAAACCTCOCTACTCC
RYR2amp3	GGTAGTAGAAGTAGAAGGTAG	CATCCTCAAAAAACACCCOCTC
RYR2amp4	GAGGGGGTGTTTTTGAGGATG	CCACCOCTACTCTACACCOCTAOC
RYR2amp5	GGTAGGGGTAGAGTAGGGTGG	CTTTCACAACACCTTAACTAAA
RYR2amp6	GGTGGGGGTGATGGTGTAGG	ACCACCOCTACCOCTTACACTTAC

<sup>1</sup> Forward primers are 5'-tagged with AGGAAAGAGAG

<sup>2</sup> Reverse primers are 5'-tagged with CAGT AAT ACCACTCACTATAGGGAGAAGGCT

**Supplemental Table S6. Correlation of Clusters with low (A), moderate (B) and high (C) RYR2 gene promoter methylation with clinical and pathological features**

Features	Category	Cluster A1		Cluster A2	
		n	%	n	%
Age [years]	<61.72	6	46,2%	19	50,0%
	>61.72	7	53,8%	19	50,0%
Gender	female	4	30,8%	8	21,1%
	male	9	69,2%	30	78,9%
Tobacco	no	3	23,1%	13	34,2%
	yes	10	76,9%	25	65,8%
Alcohol	no	7	53,8%	20	52,6%
	yes	6	46,2%	18	47,4%
HPV-related	no <sup>1</sup>	13	100,0%	29	76,3%
	yes <sup>2</sup>	0	0,0%	9	23,7%
Subsite	Larynx/Hypopharynx	1	7,7%	11	28,9%
	Nasal cavity	4	30,8%	2	5,3%
	Oral cavity	5	38,5%	11	28,9%
	Oropharynx	3	23,1%	14	36,8%
Tumor size	T1-2	4	30,8%	16	42,1%
	T3-4	9	69,2%	23	60,5%
Lymph node metastasis	N0	7	53,8%	13	34,2%
	N+	6	46,2%	25	65,8%
Pathological grading	G1-2	10	76,9%	26	68,4%
	G3	3	23,1%	12	31,6%
Resection margin	R0	10	76,9%	32	84,2%
	R1	3	23,1%	6	15,8%
	R2	0	0,0%	0	0,0%
Therapy	S	3	23,1%	11	28,9%
	SRT	6	46,2%	13	34,2%
	SRCT	4	30,8%	14	36,8%

<sup>1</sup>DNA negative or DNA positive but RNA negative; <sup>2</sup>DNA and RNA positive; S=surgery; RT=adjuvant radiotherapy; RCT=adjuvant radiotherapy

<sup>3</sup>Chisquare test; significant differences are indicated in bold

2 gene promoter

Cluster B		
n	%	p value <sup>3</sup>
11	52,4%	0,94
10	47,6%	
3	14,3%	0,516
18	85,7%	
6	28,6%	0,733
15	71,4%	
9	42,9%	0,737
12	57,1%	
9	42,9%	<b>0,001</b>
12	57,1%	
3	14,3%	<b>0,005</b>
1	4,8%	
2	9,5%	
15	71,4%	
12	57,1%	0,259
9	42,9%	
4	19,0%	0,111
17	81,0%	
11	52,4%	0,289
10	47,6%	
13	61,9%	0,155
8	38,1%	
1	4,8%	0,226
8	38,1%	
12	57,1%	

radiochemotherapy

Supplementary Table S7 is available in: <https://onlinelibrary.wiley.com/doi/full/10.1002/ijc.32481>



## 5. CONCLUSION

Presently, no validated biomarkers exist to identify HNSCC patients with a higher probability for treatment failure who would benefit from closer follow-up and different therapeutic approaches. The current standard therapies for HNSCC are either rather toxic or have low response rates. In order to improve patient survival and reduce treatment-related toxicity, the identification of biomarkers is urgently needed. The establishment of reliable biomarkers would allow for the potential to identify patients at high risk for tumor relapse and could be extremely beneficial for treatment decision making.

Considering HNSCC heterogeneity, the analysis of combined multiple genes and/or DNA alterations may provide a better coverage for biomarker detection. In this study, the combination of genetic and epigenetic alterations showed the effect of DNA methylation in regulating two different genes (RYR2 and SOX2) during tumor initiation and progression. The detection of DNA methylation and respective gene expression might help to predict patients risk for malignant transformation and worse outcome. In a near future, scientific advances on DNMT inhibitors and DNA methylation may lead to a transition from cytotoxic to targeted therapies that could reverse the cancer cells back to a more normal-like state, improving clinical success.

Recent studies have shown that epigenetic switch between SOX2 and SOX9 is regulated to cell plasticity (LIN et al., 2016) immune evasion (MALLADI et al., 2016) and induced drug resistance (SHARMA et al., 2018). Future studies exploring the combination of different regulatory mechanisms and SOX2-related genes might help to better understand tumor complexity.

Pilot studies from our laboratory have shown that RYR2 is positive in highly mobile tumor cells *in vitro* and has greater expression in tumor invasion areas when compared to the center of the tumor. This, added to controversial finding in literature regarding RYR2 expression, suggests a context-dependent function of RYR2 that needs to be further explored.

To better describe the profile of invasive cells regarding RYR2 and SOX2 expression, genetic and epigenetic alterations, gene-related and drug resistance, a more sophisticated tool that preserves the biological features of the original source and connects lab and clinical practices is needed. Three-dimensional (3D) models have been proven to better reflect environmental cues and mimic patho-physiological processes: cell-cell, cell-matrix interactions and cross-talk, *in vivo* growth, differentiation and dedifferentiation conditions. The 3D spheroid model has showed to be an adequate cost/benefit biotechnological tool to assess tumor cell invasion mechanisms, to investigate drug response and improve personalized medicine.

LIN S.C., CHOU Y.T., JIANG S.S., CHANG J.L. et al. Epigenetic Switch between SOX2 and SOX9 Regulates Cancer Cell Plasticity. *Cancer Research*. 76(23):7036-7048. Dec 1; 2016

MALLADI S., MACALINAO D.G., JIN X., HE L. et al. Metastatic Latency and Immune Evasion through Autocrine Inhibition of WNT. *Cell*. 165(1):45-60. Mar 24; 2016.

SHARMA A., CAO E.Y., KUMAR V., ZHANG X. et al. Longitudinal single-cell RNA sequencing of patient-derived primary cells reveals drug-induced infidelity in stem cell hierarchy. *Nature Communication*. 22;9(1):4931. Nov 22 2018-